

Long-term variability of corona, solar wind and IMF

Kalevi Mursula

Space Climate group

Space physics and Astronomy research unit
University of Oulu

kalevi.mursula@oulu.fi

Outline

Photosphere

Sunspots, active regions and TSI

Photospheric magnetic field

Corona

PFSS model

Solar wind

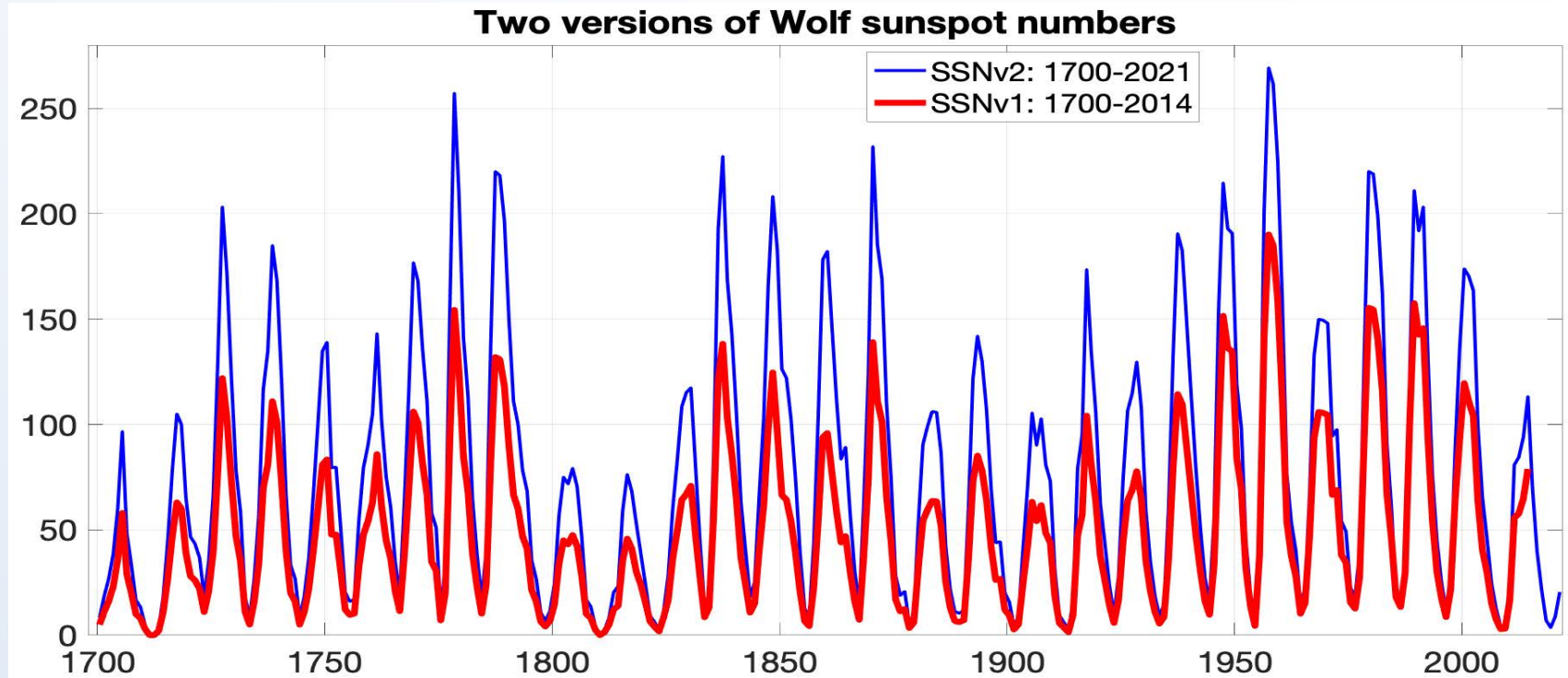
Heliospheric magnetic field

HCS

Photosphere

Sunspots, active regions and TSI

Wolf sunspot numbers since 1700



Main features of sunspot activity since 1700:

- Solar 11-year cycle, Gleissberg cycle
- Grand Modern Maximum in mid-1900s (GMM)
- WEAK CYCLE 24 which ends the GMM !

Sunspot number status

Several **inhomogeneities** found in original (version 1) Wolf and group sunspot number series.

Version 2 of Wolf numbers launched in 2015.

However: No consensus yet on sunspot numbers !

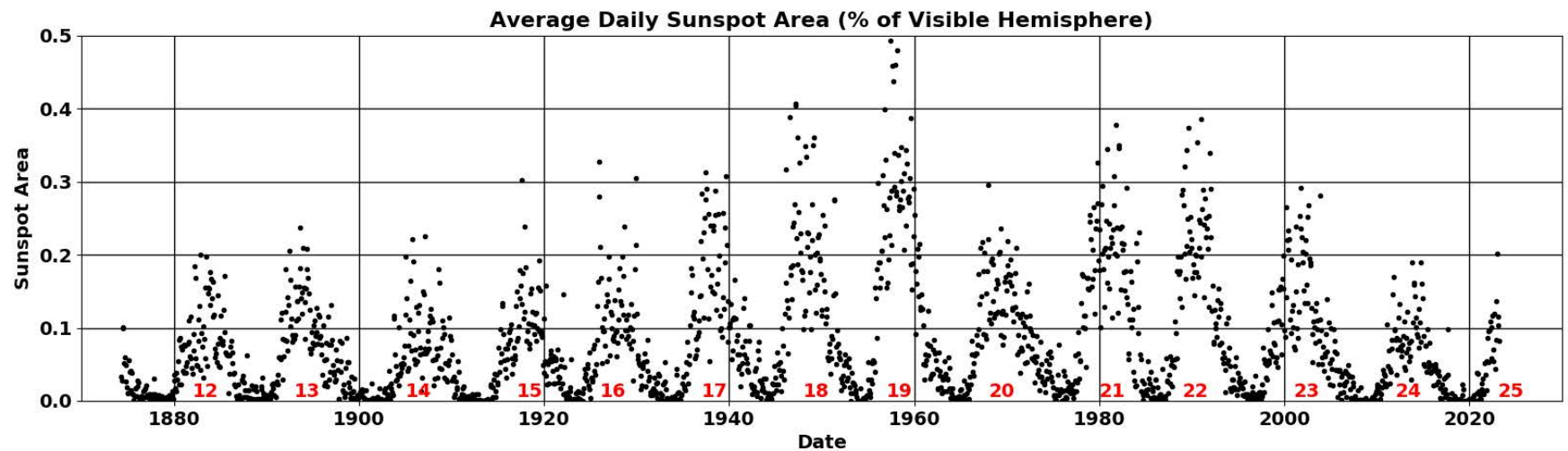
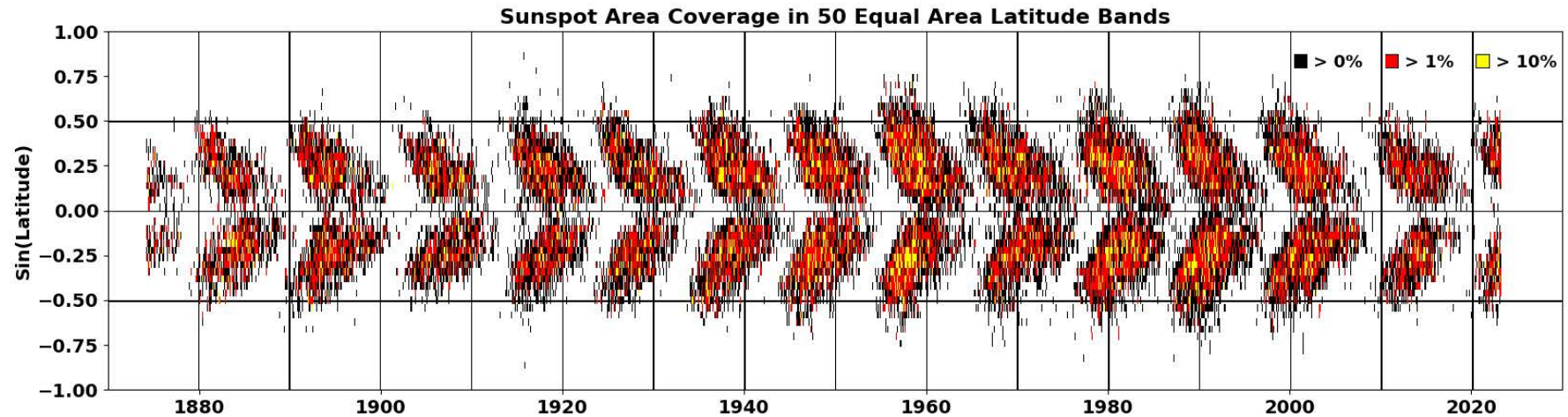
- Debate on the relative level of activity maxima in the last 300 years and the relative height of the Grand Modern Maximum.
- New reconstructions under way.
- The standard comparison of observers (via coefficients k) will be revised.

We know now how **partial information** sunspots yield about solar magnetic fields.

Even worse: Sunspot numbers are **unscientific** figures, largely based on trusting the good judgement of the early observers (and R. Wolf).

Aim: Make sunspots scientific by reliable (time dependent) error estimates.

Sunspot "butterfly" occurrence



<http://SolarCycleScience.com>

2023/05 Hathaway

Active regions and eruptions

Active regions (AR) are regions of enhanced magnetic fields.

In photosphere they are seen, e.g., as **faculae and sunspots**.

In corona they form large **coronal loops** connecting points of opposite magnetic polarity in the photosphere.

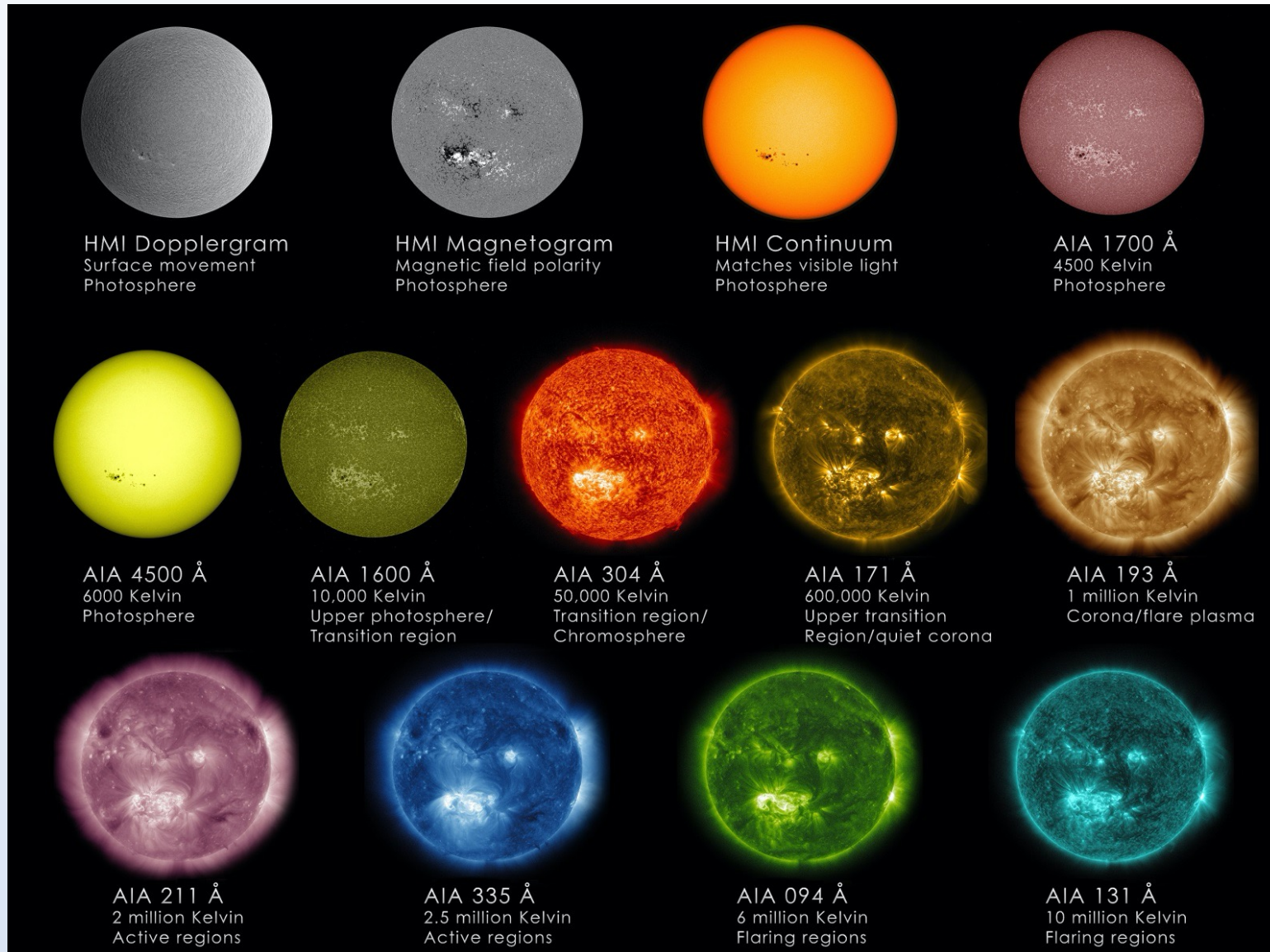
- Coronal loops gather large amounts of plasma. Due to enhanced absorption they are seen as dark regions (so called **filaments**) on solar surface and, due to enhanced reflection, as bright regions at solar limb (so called **prominences**).

Coronal mass ejections (CME) are eruptions of large coronal loops.

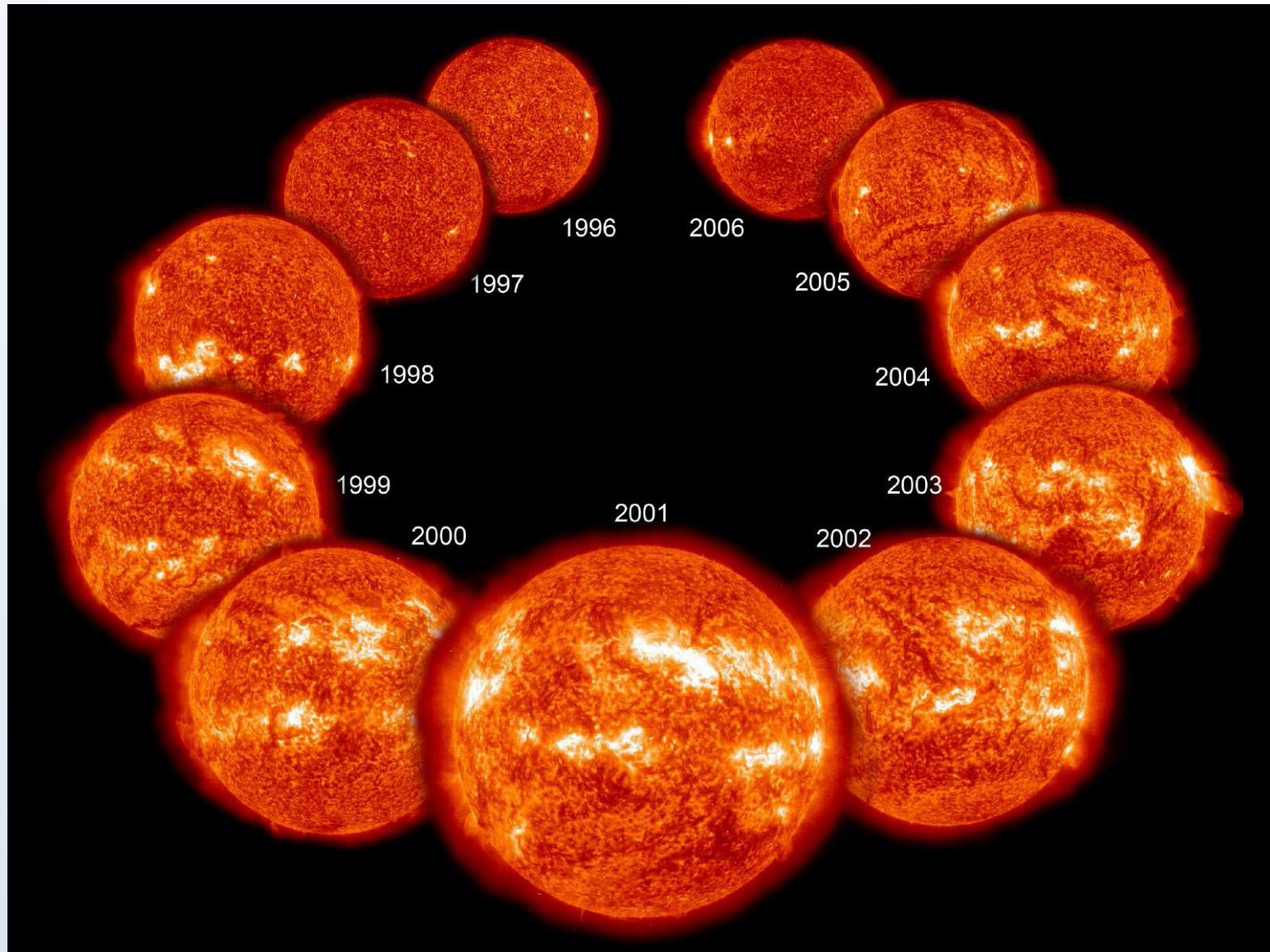
- As all magnetic activity, CMEs maximize at solar maxima.
- CMEs cause the largest disturbances in the near-Earth space.

Flares are smaller-scale eruptions occurring in active regions. They are characterized by a sudden increase of X-rays and solar energetic particles.

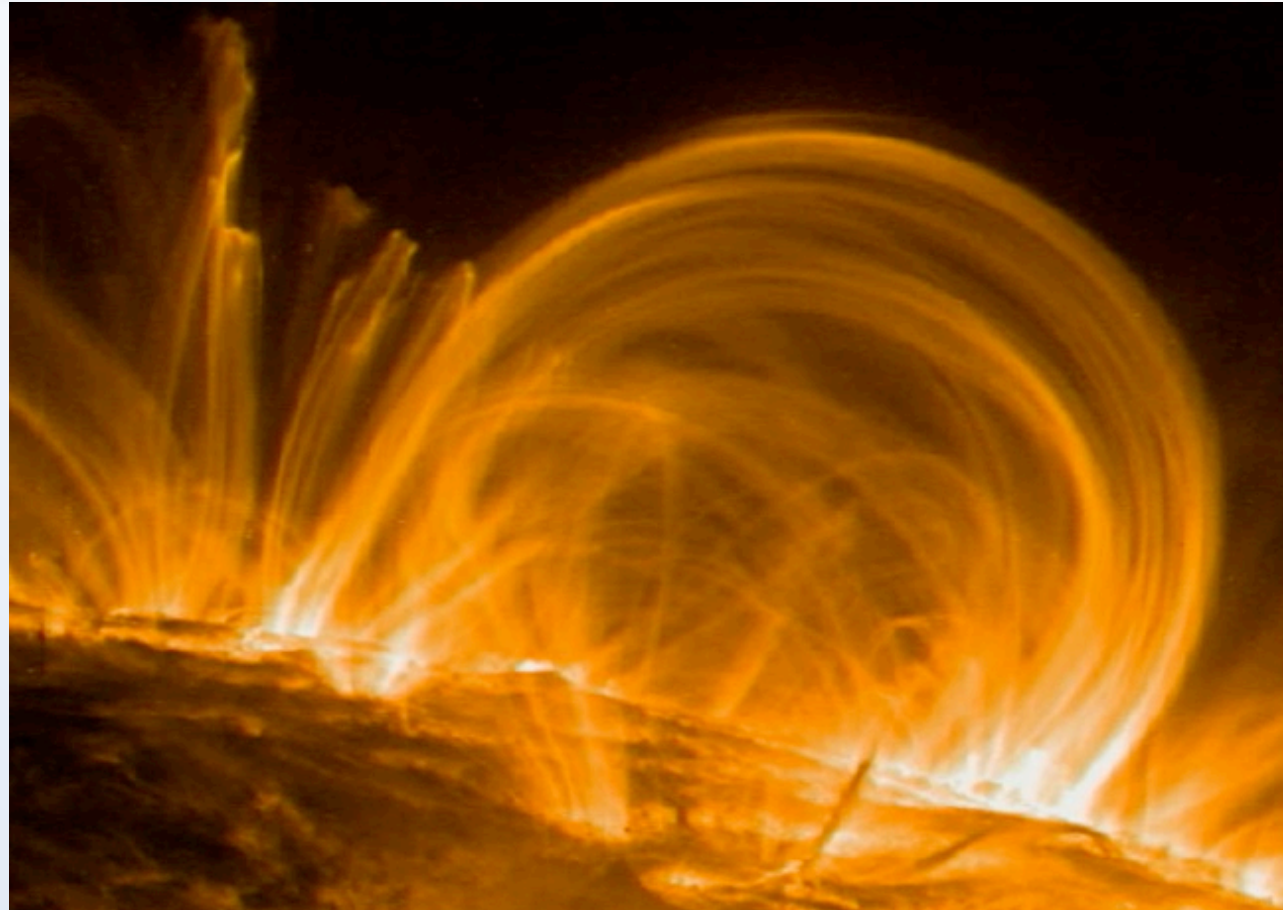
Sun at different (SDO) wavelengths



Solar cycle at 304Å EUV (active regions)



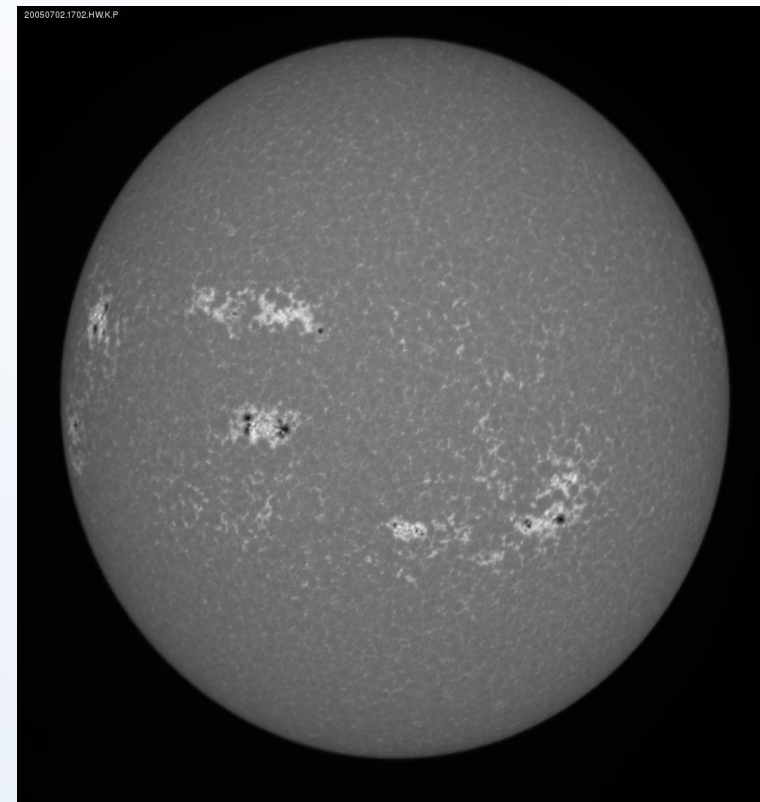
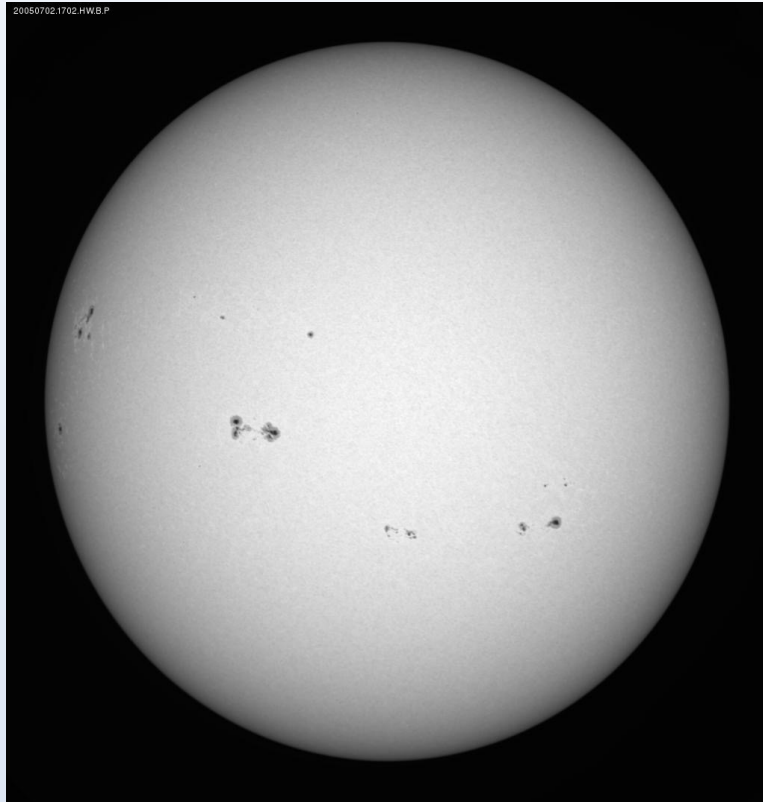
Magnetic field structure from observed radiation



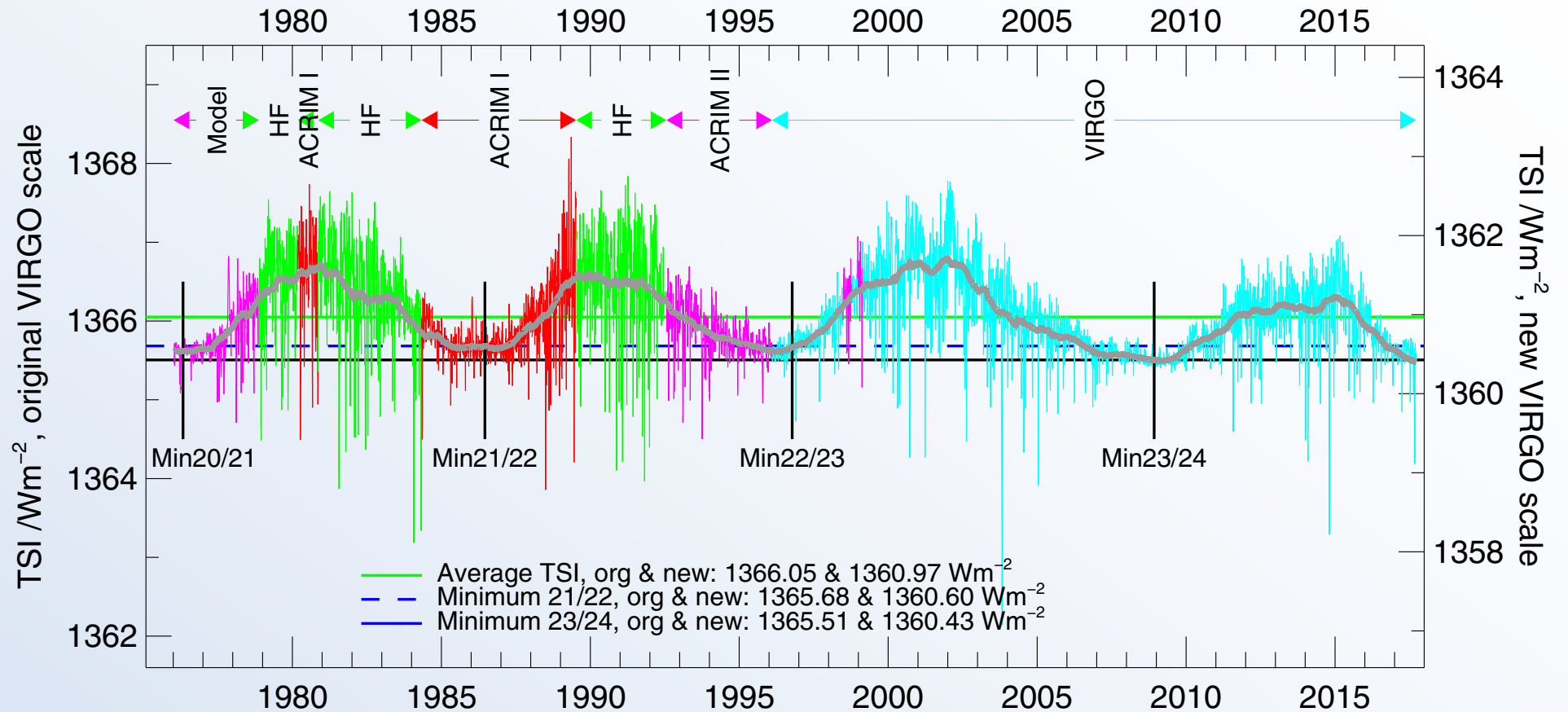
Detailed view of coronal plasma measured by the Trace satellite, depicting magnetic loops in active regions.

Intensity of emitted radiation reflects the density of the region.

Sunspots and faculae (active regions in white light)



TSI: PMOD series



TSI: PMOD series

Total Solar Irradiance has been measured on satellites since 45 years

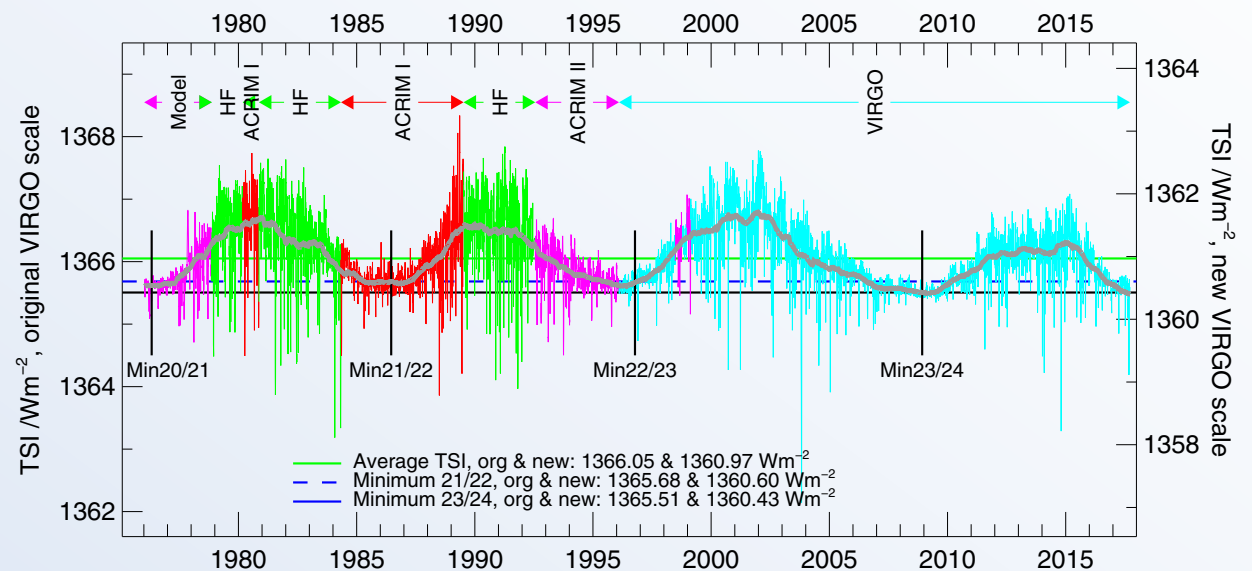
Solar cycle **in-phase variation** with 0.1% amplitude.

Sunspots reduce TSI

Faculae overcompensate that.

TSI cycle amplitudes **follow the decrease** of sunspot cycle amplitude.

No verified trend of TSI at sunspot minima.



TSI: Faculae

TSI is stronger during high sunspot number years than during solar minima.

This seems contradictory to the cooling effect of sunspots!

Solution: Faculae, bright spots.

Faculae are small (about 0.25" diameter, smaller than granular size) but they are many. Their **total area** is 15-20 times larger than the area covered by sunspots. A sunspot group is typically surrounded by a large region of faculae.

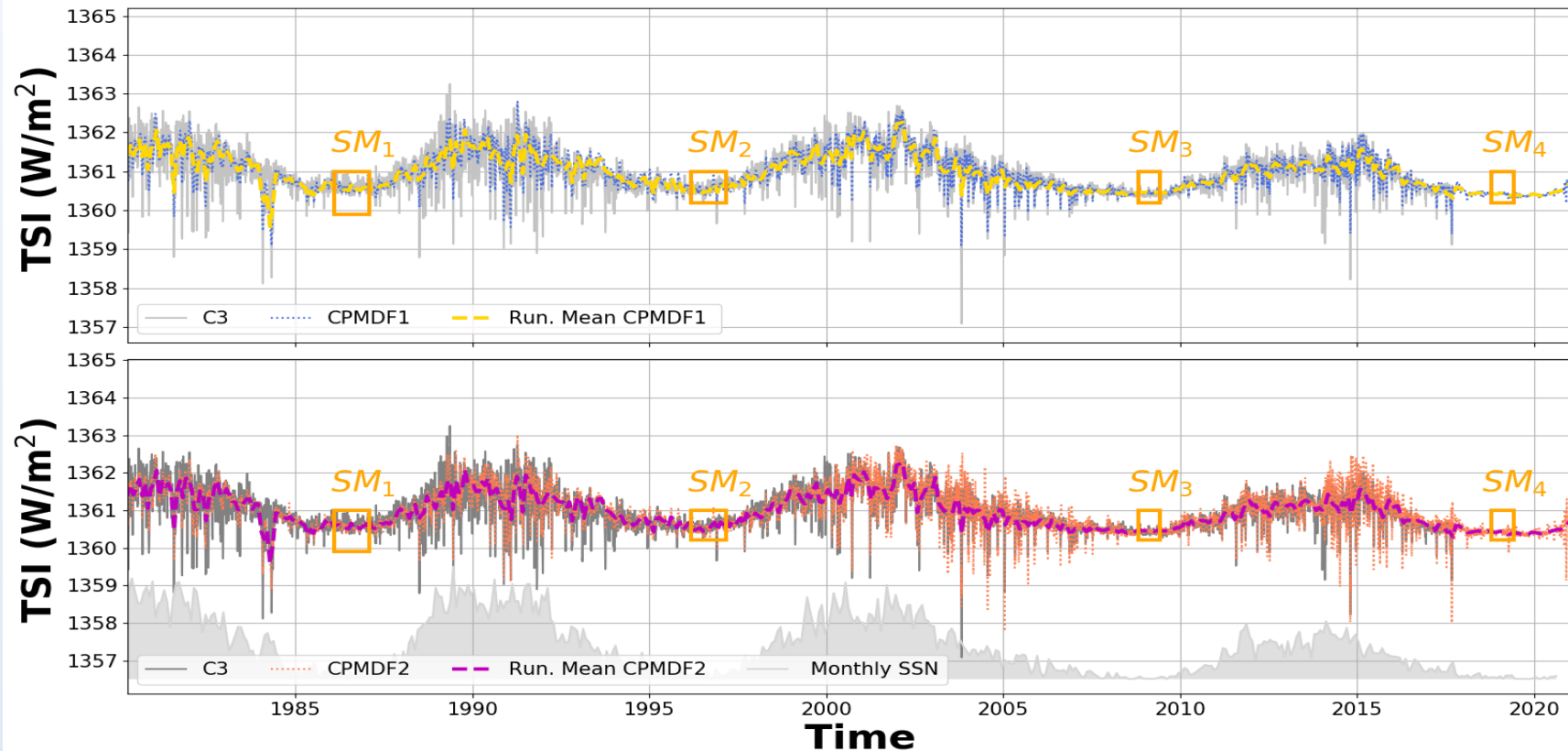
Facular brightness can overcompensate the dimming due to sunspots.

Faculae are also magnetically active regions with moderate strength (about 0.01 T).

Therefore the number of faculae increases with increasing average magnetic activity.

= > TSI correlates with sunspots (thanks to faculae).

TSI: PMOD series



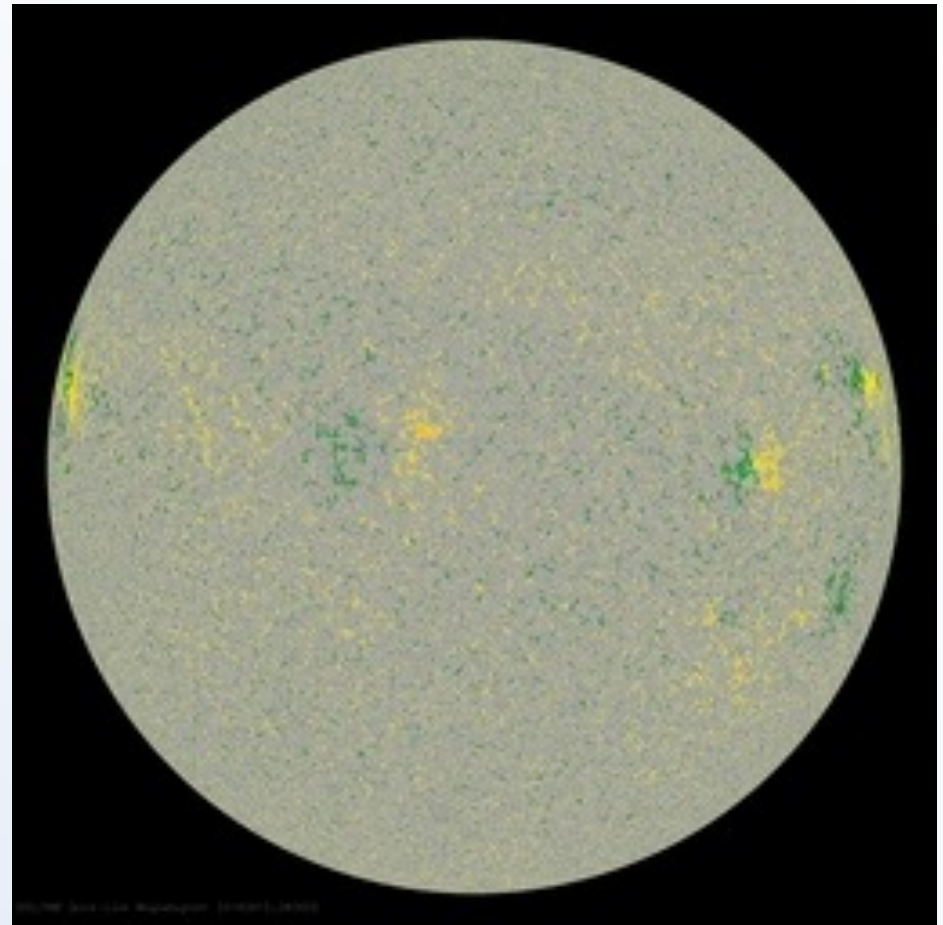
New 41-year TSI composite without (CPMDF1 at top; blue) and with a wavelet filter (CPMDF2 at bottom; orange). For comparison, C3 (Fröhlich, 2006) is shown (grey line). 30-day running mean of CPMDF1 is shown as a yellow/purple dashed line. Orange boxes are associated with solar minima (SM).

Photosphere

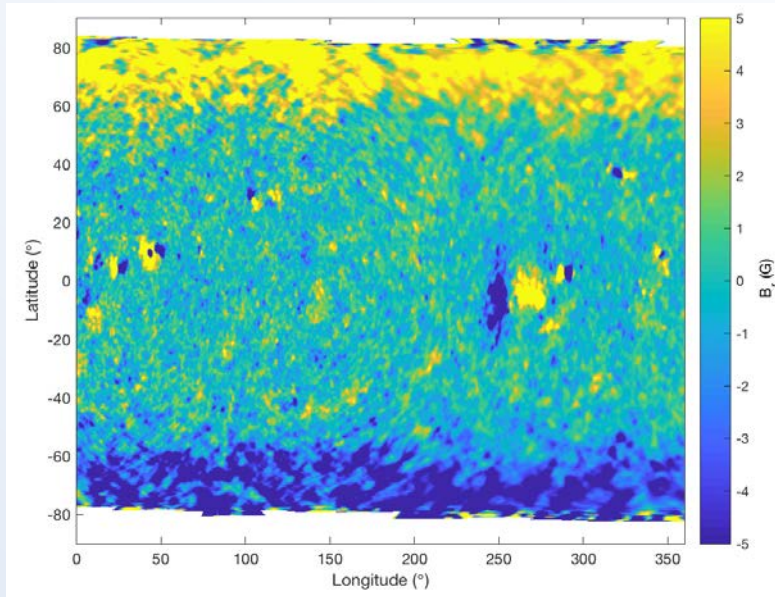
Photospheric magnetic field

Photospheric magnetic field

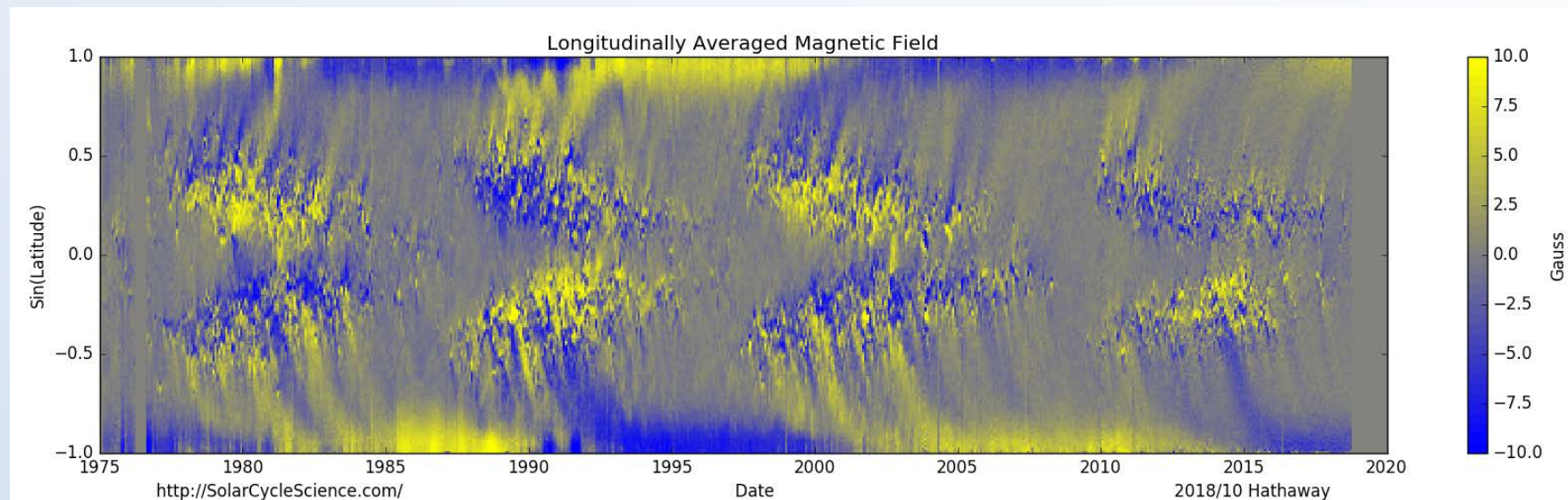
- Solar magnetic field is generated by the solar dynamo in the convection zone.
- **All surface** is magnetic, not only sunspots or active regions.
- Photospheric magnetic field is complicated, with more and more details appearing with improved resolution.
- **Small scale fields produce most of the total flux.**



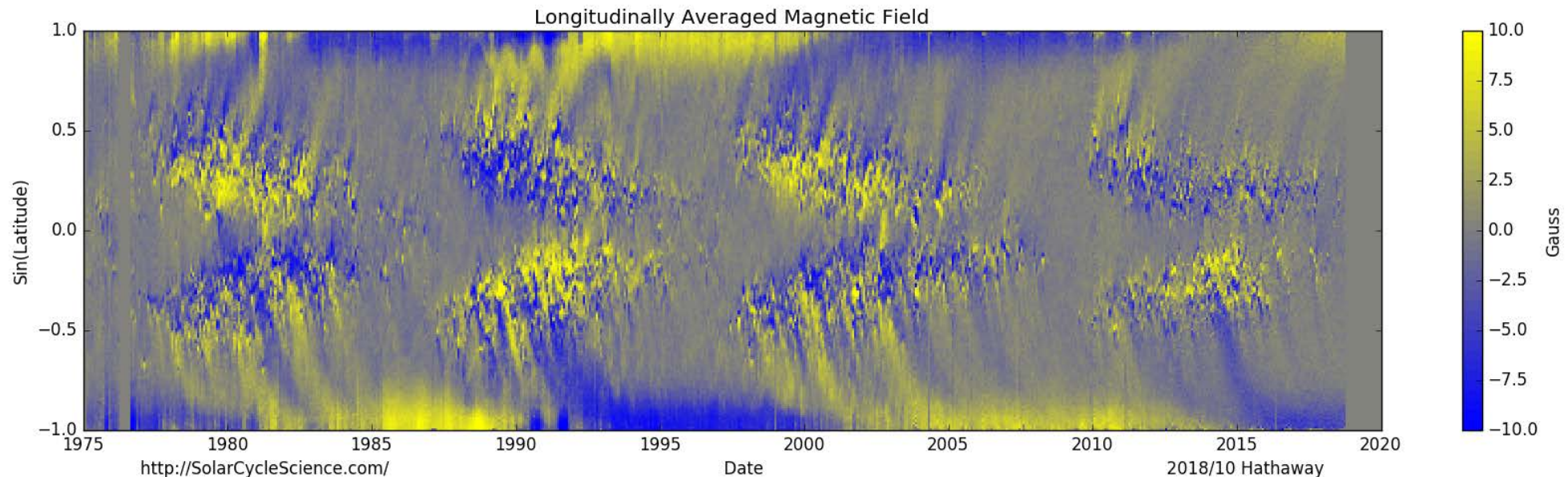
Synoptic and supersynoptic maps of the photospheric magnetic field



The measured photospheric magnetic field is often represented as a **synoptic map** (left) or a longitude-averaged combination of them called the **supersynoptic map**.

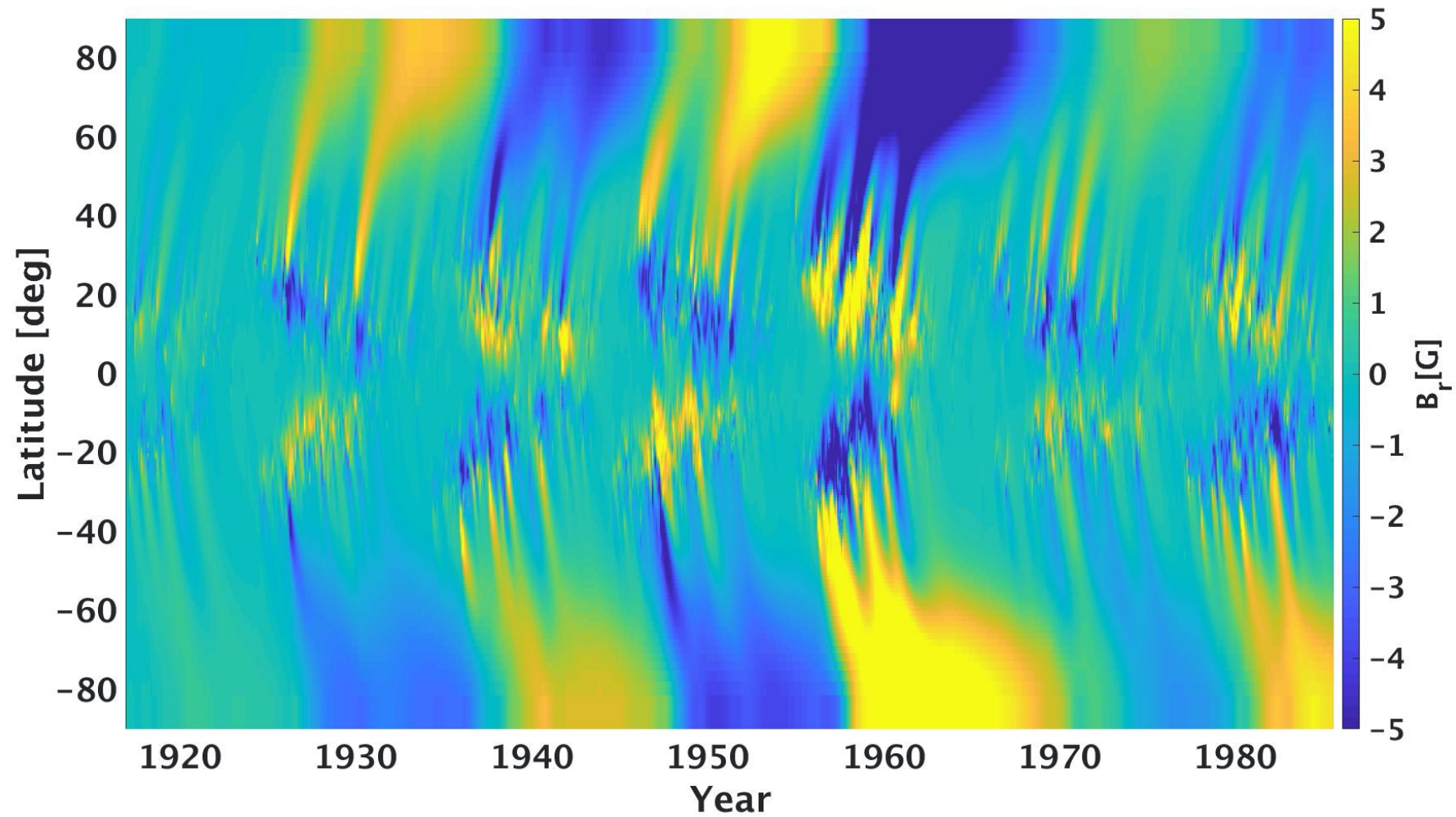


Photospheric magnetic field



- Magnetic flux is generated at low to mid-latitudes and transported by **poleward** (mainly **trailing** flux) and **equatorward** (mainly **leading** flux) surges.
- Polar field **reversals** caused by poleward surges.

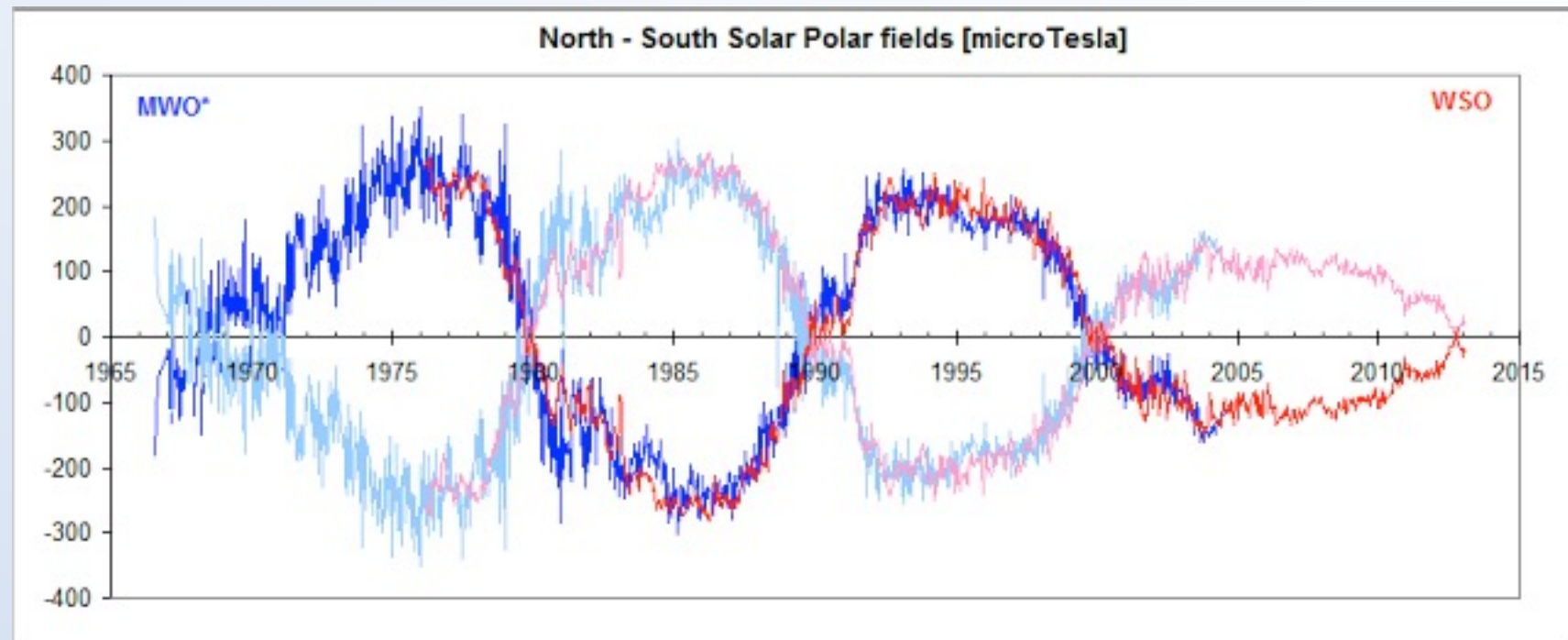
Centennial SFT simulation



Polar field evolution

Direct measurements of solar polar field only since 1970s

Polar field decreases since 1970s. **Large drop from 1990s to 2000s**

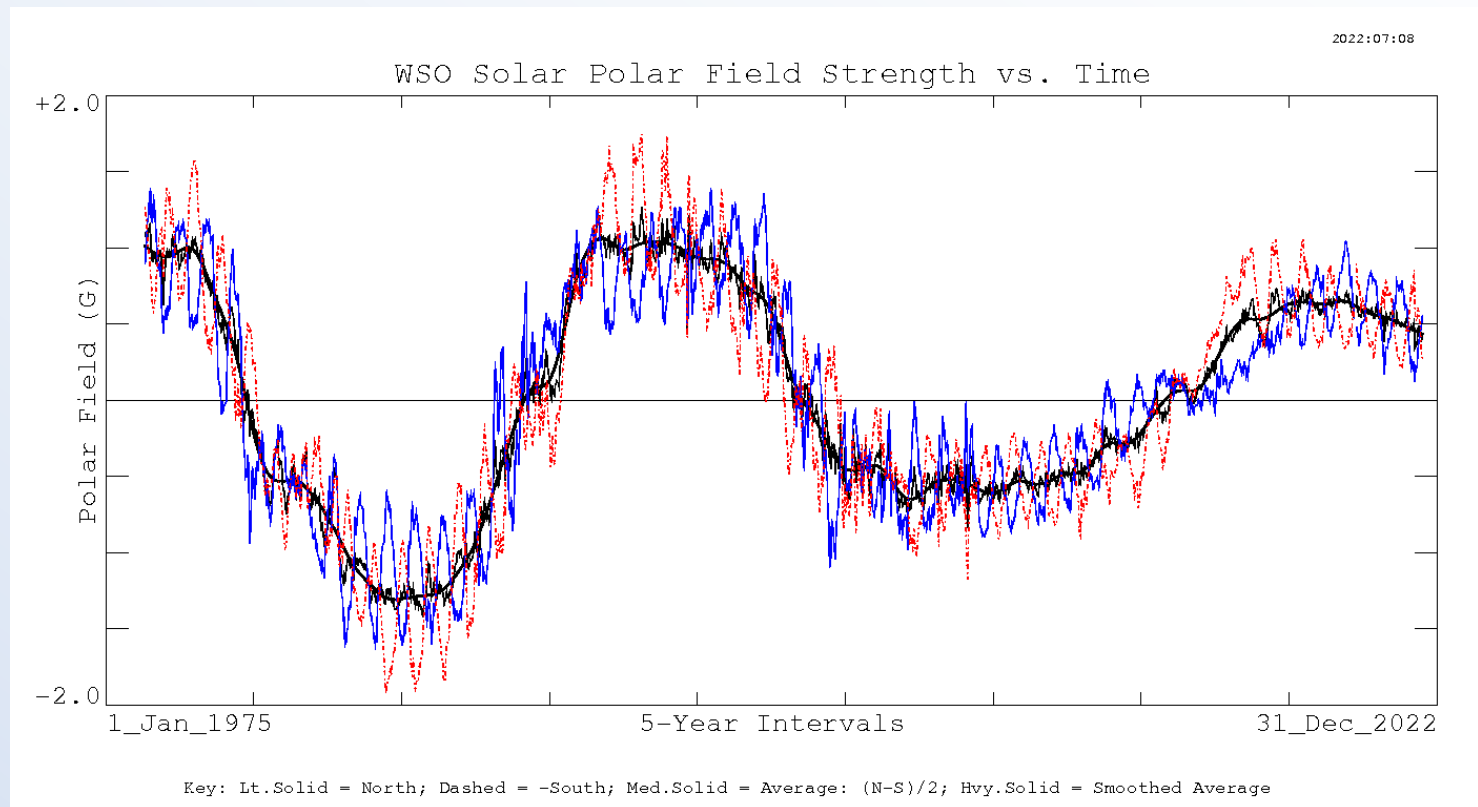


Polar field evolution: N and S

South field sign is reversed here for better comparison with N.

Decline of intensity continues until SC24.

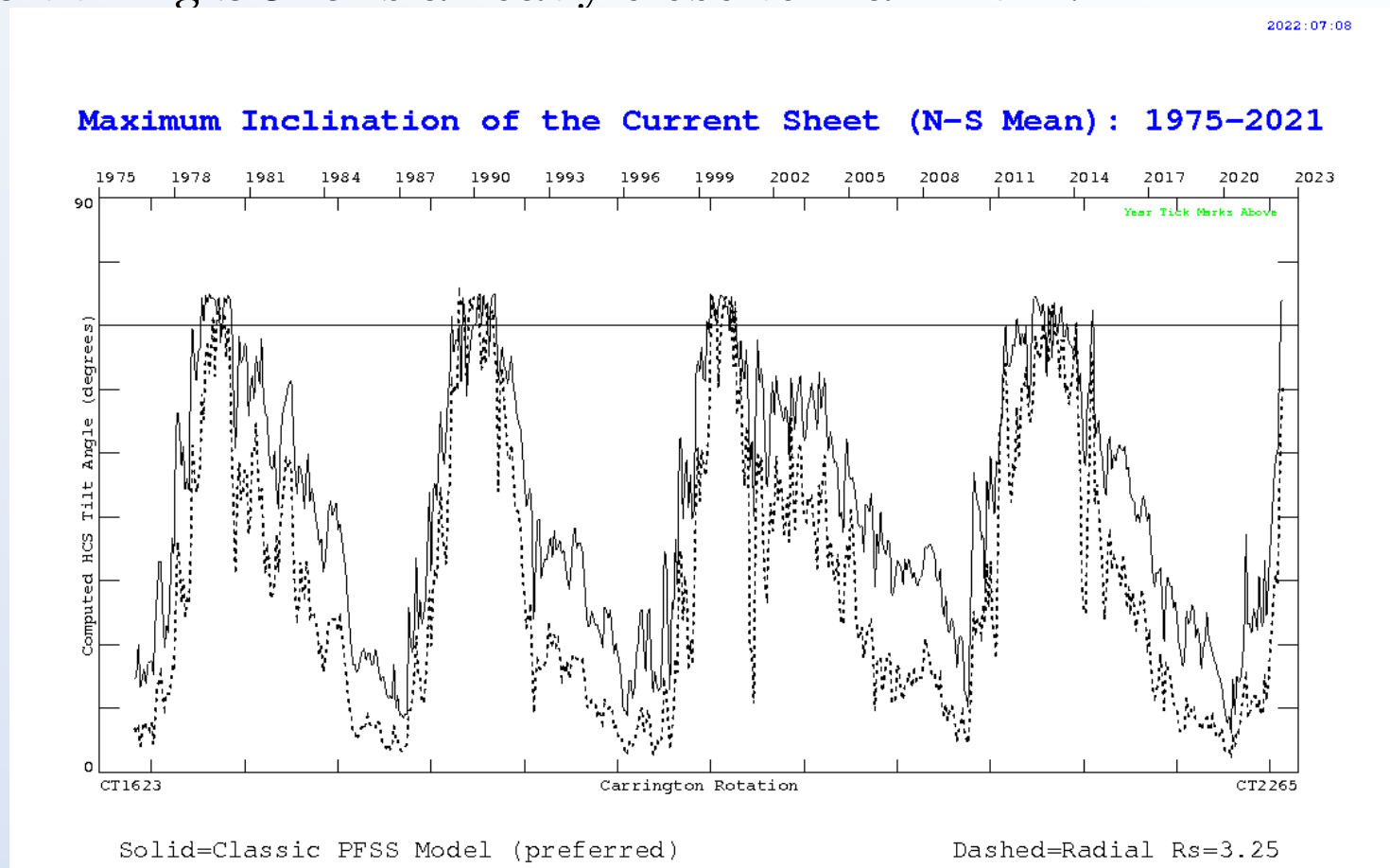
South field maximum is always **larger** than North (**Bashful ballerina**)



Polar field evolution: Dipole tilt

Dipole tilt (HCS inclination) is low at solar minima and large at solar maxima.

HCS during SC25 is already close to maximum.

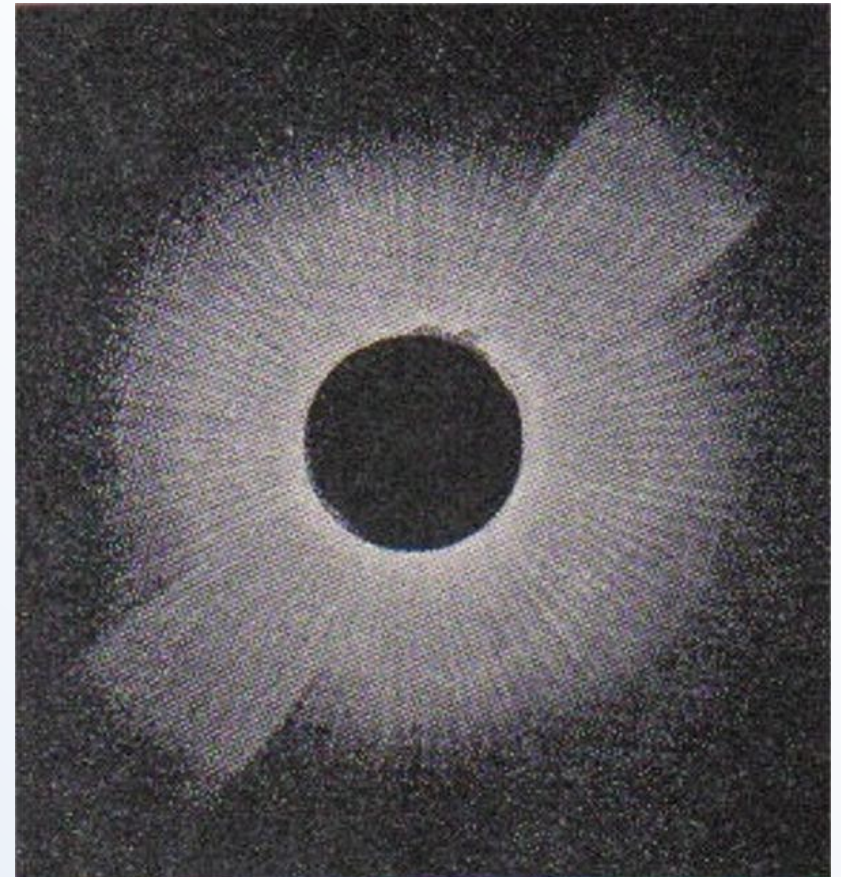


Corona

Coronal observations, solar eclipse in 1842

Tilted, flat HCS (streamer belt) in 1842.

This is a **typical** structure for the **declining phase** of the solar cycle



Coronal observations, solar eclipses in 1929, 1932, 1934

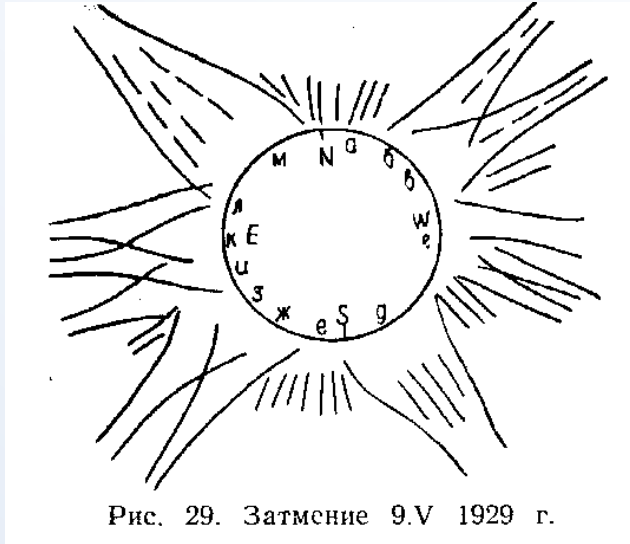


Рис. 29. Затмение 9.V 1929 г.

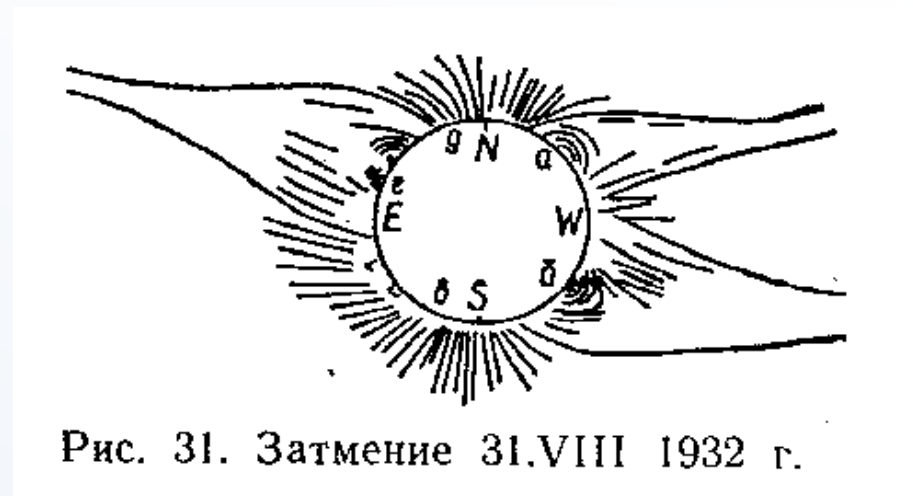


Рис. 31. Затмение 31.VIII 1932 г.

These drawings (in Russian) during successive eclipses depict the **transformation of coronal** (and heliospheric) **structure** from solar maximum in 1929 via the declining phase in 1932 to solar minimum in 1934.

Streamers and **coronal holes** are visible.

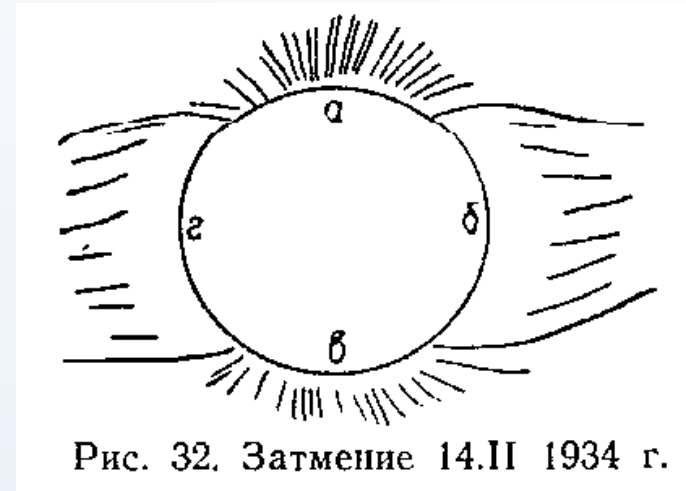
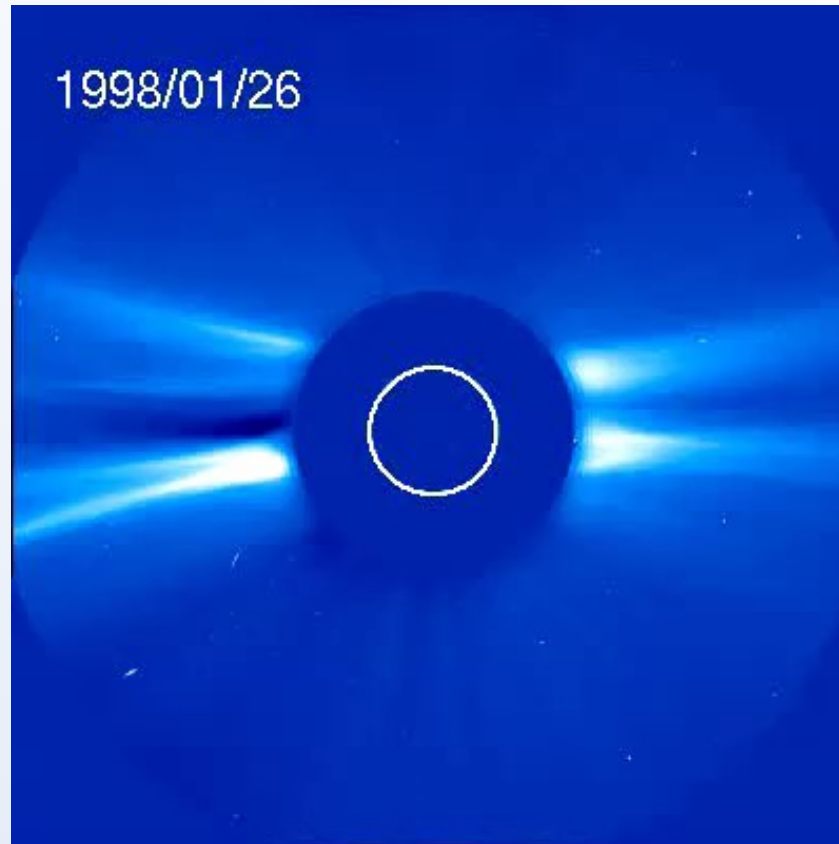


Рис. 32. Затмение 14.II 1934 г.

Coronagraphs: SOHO LASCO C2



Corona is here observed by LASCO C2 in 1998 over 1 month between January 26 and February 26. The cadence is about 1 image per hour. Note the effect of solar rotation on the location of the streamers (and CMEs).

Corona: Streamers and holes

Coronal holes (CH) are areas where the solar corona (when seen in white light) looks dark (there is little reflected light).

- Coronal holes occur when the solar **magnetic field is open** to interplanetary space.
- CHs are sources of **fast solar wind**.

Polar coronal holes (PCH) are formed in the declining phase.

- PCH dominate the solar coronal magnetic field around solar minima.
- PCH make extensions to lower latitudes in the declining phase.
- These are important as they are sources of fast SW reaching the Earth.

Streamers are regions of dense coronal plasma.

- Streamers are related to active regions that form closed loops.

The main streamers form the **heliospheric current sheet** (HCS).

- HCS is the solar **magnetic equator in space**, separating the two solar hemispheres of opposite polarity.
- HCS is quite flat during solar minima but tilted and warped at other times.

Coronal holes

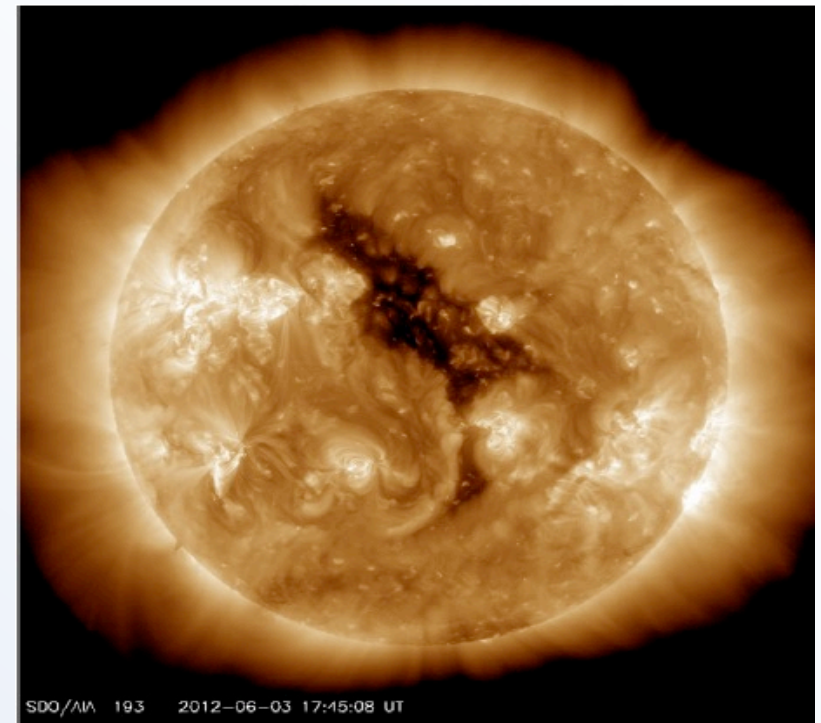
Coronal holes are seen as long-lived **regions of low intensity** both in scattered coronal light (in white light or line emissions) and emitted coronal light (coronal spectral line emissions in visible, UV or X-ray radiation).

The low emission from coronal holes means that these are regions of **low coronal plasma density**.

Coronal holes are **unipolar magnetic field regions** of open magnetic flux.

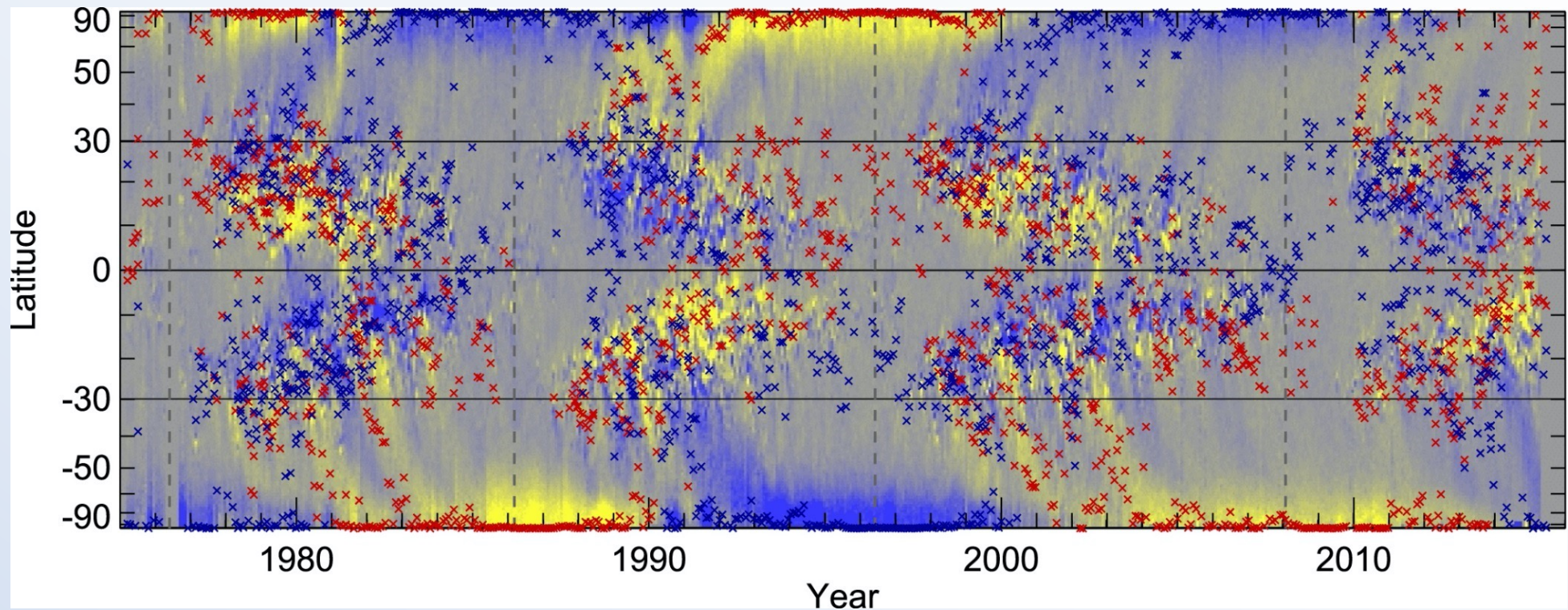
Coronal holes are sources of **fast solar wind** flows ($V_{sw}=700-800\text{km/s}$).

The unipolar magnetic structure and the fast SW outflow reduce the coronal density in coronal holes.



Coronal holes

- CH location varies over the solar cycle
- CHs follow surges of the magnetic field from mid-latitudes to the poles
- Large unipolar CH regions at the poles during most of the solar cycle



Blue dots show coronal holes with negative polarity, red dots with positive polarity.

Corona

Coronal magnetic field and PFSS

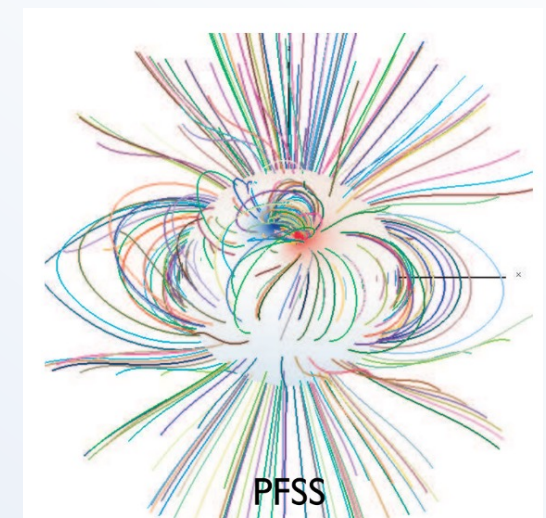
Coronal magnetic field: Great unknown

- Coronal magnetic field defines the heliospheric magnetic field structure beyond the solar system.
- Therefore coronal field is highly important for **space weather and space climate** studies.
- Coronal magnetic field has **not** been measured over long time intervals. **Need modeling!**



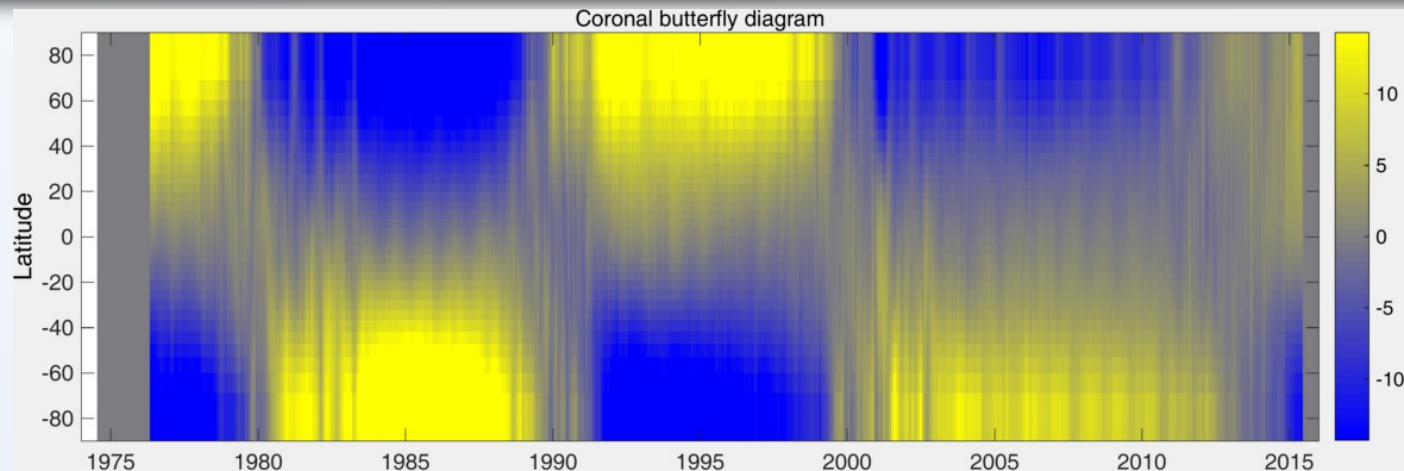
Solar eclipse in 2008

- One often uses the PFSS model, which assumes current-free corona and radial magnetic field at few solar radii (source surface).
- Source surface radius is the **only free parameter** of the PFSS model.
- Field lines reaching the source surface radius open into the heliosphere
=> **The smaller R_{SS} the larger the open flux.**

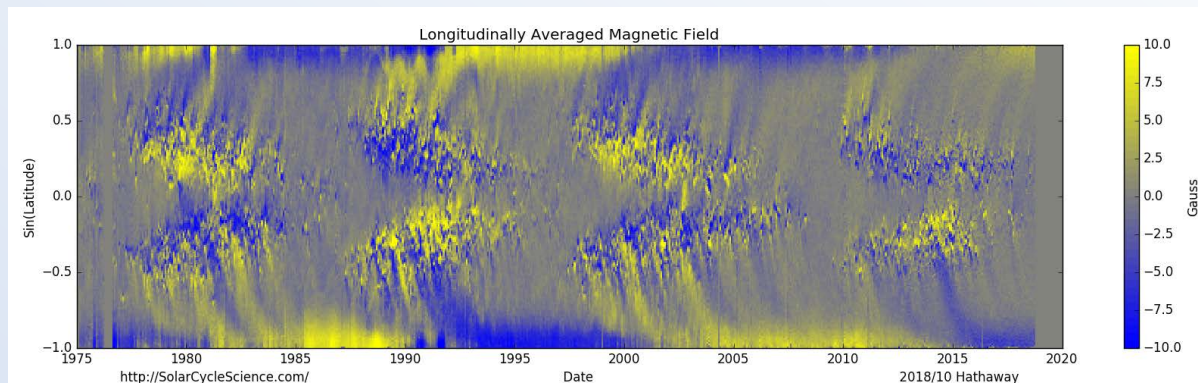


From Riley et al., 2007

Coronal magnetic field



- Much **simpler magnetic structure** in coronal source surface (above) than in the photosphere (below).
- Coronal field is dominated by **lowest harmonic terms**, the axial and equatorial dipoles, over most of the cycle, especially during solar minima.
- More complex structure only during 1-2 years around solar maxima.



Current-free corona: Laplace eq.

Altschuler and Newkirk (1969) and Schatten et al. (1969):

No electric currents between photosphere and corona:

$$\nabla \times \mathbf{B} = 0 \Rightarrow \mathbf{B} = -\nabla \Psi$$

Together with Gauss' law $\nabla \cdot \mathbf{B} = 0$ we get the Laplace equation:

$$\nabla^2 \Psi = 0$$

Solution for $\Psi(r, \theta, \phi)$ is obtained as an **expansion**:

$$\Psi(r, \theta, \phi) = R_S \sum_{n=0}^{\infty} \sum_{m=0}^n R_n(r) P_n^m(\cos\theta) (g_{nm} \cos m\phi + h_{nm} \sin m\phi)$$

in terms of **spherical harmonic functions** $P_n^m(\cos\theta) \cos m\phi$ and $P_n^m(\cos\theta) h_{nm} \sin m\phi$ which describe the **angular dependence on a sphere**, and the radial function R_n .

PFSS model

The PFSS model assumes that the **field is radial in the upper corona**, at the distance called the **source radius** r_{SS} .

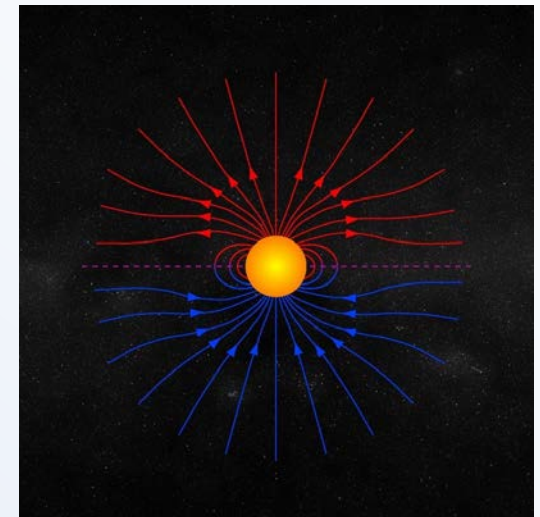
Then the radial function in the potential can be solved and the PFSS solution for $\Psi(r, \theta, \phi)$ in terms of spherical harmonics is

$$\Psi(r, \theta, \phi) = R_S \sum_{n=0}^{\infty} \sum_{m=0}^n P_n^m(\cos\theta) (g_{nm} \cos m\phi + h_{nm} \sin m\phi) \times \left(\frac{R_S}{r}\right)^{n+1} \frac{1 - \left(\frac{r}{r_{SS}}\right)^{2n+1}}{n+1 + n\left(\frac{R_S}{r_{SS}}\right)^{2n+1}}$$

where

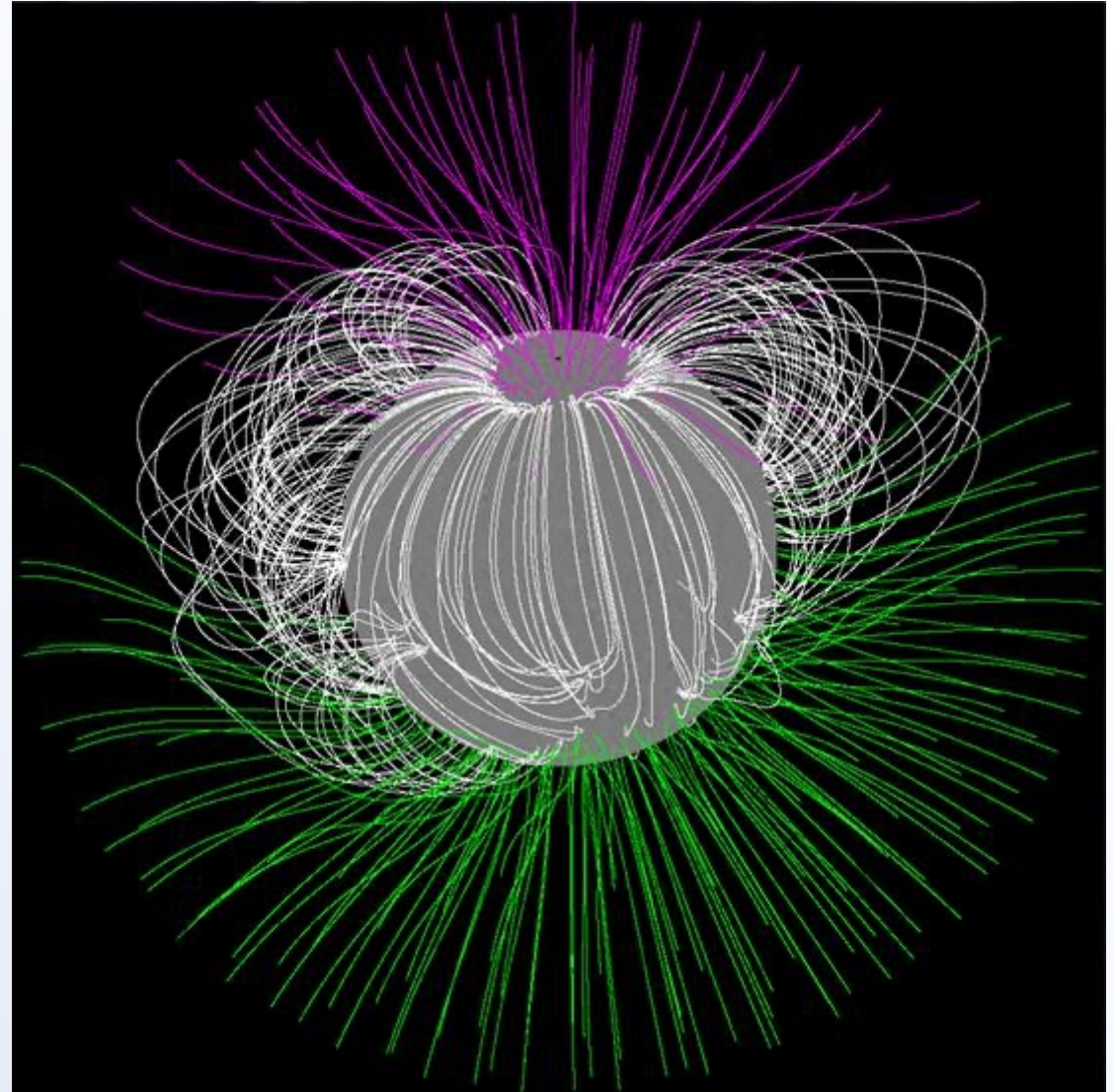
$$g_{nm} = \frac{2n+1}{N_X N_Y} \sum_{i=1}^{N_X} \sum_{j=1}^{N_Y} B_r(R_S, \theta_i, \phi_j) P_n^m(\cos\theta_i) \cos m\phi_j$$
$$h_{nm} = \frac{2n+1}{N_X N_Y} \sum_{i=1}^{N_X} \sum_{j=1}^{N_Y} B_r(R_S, \theta_i, \phi_j) P_n^m(\cos\theta_i) \sin m\phi_j$$

Beyond the source surface the solar wind plasma dominates the magnetic field \rightarrow the field is not potential-field there.



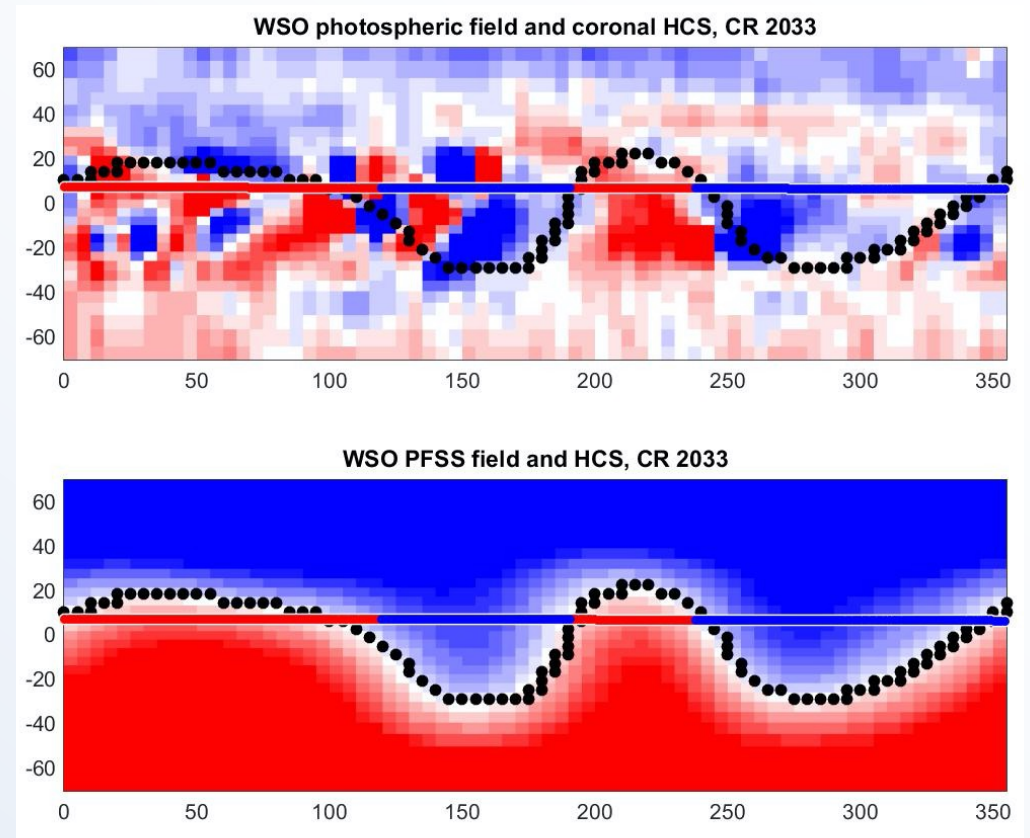
PFSS field

- Configuration of the coronal magnetic field derived from the PFSS model.
- Green and purple indicate open field lines (Toward and Away polarities) and white field lines are closed.
- Field is drawn only up to the source surface distance, where it is radial.
- PFSS model was **developed already in late 1960s**, but it is still widely used and can predict the coronal structure as well as more complicated models (like MHD models).



PFSS: Photosphere and coronal source surface

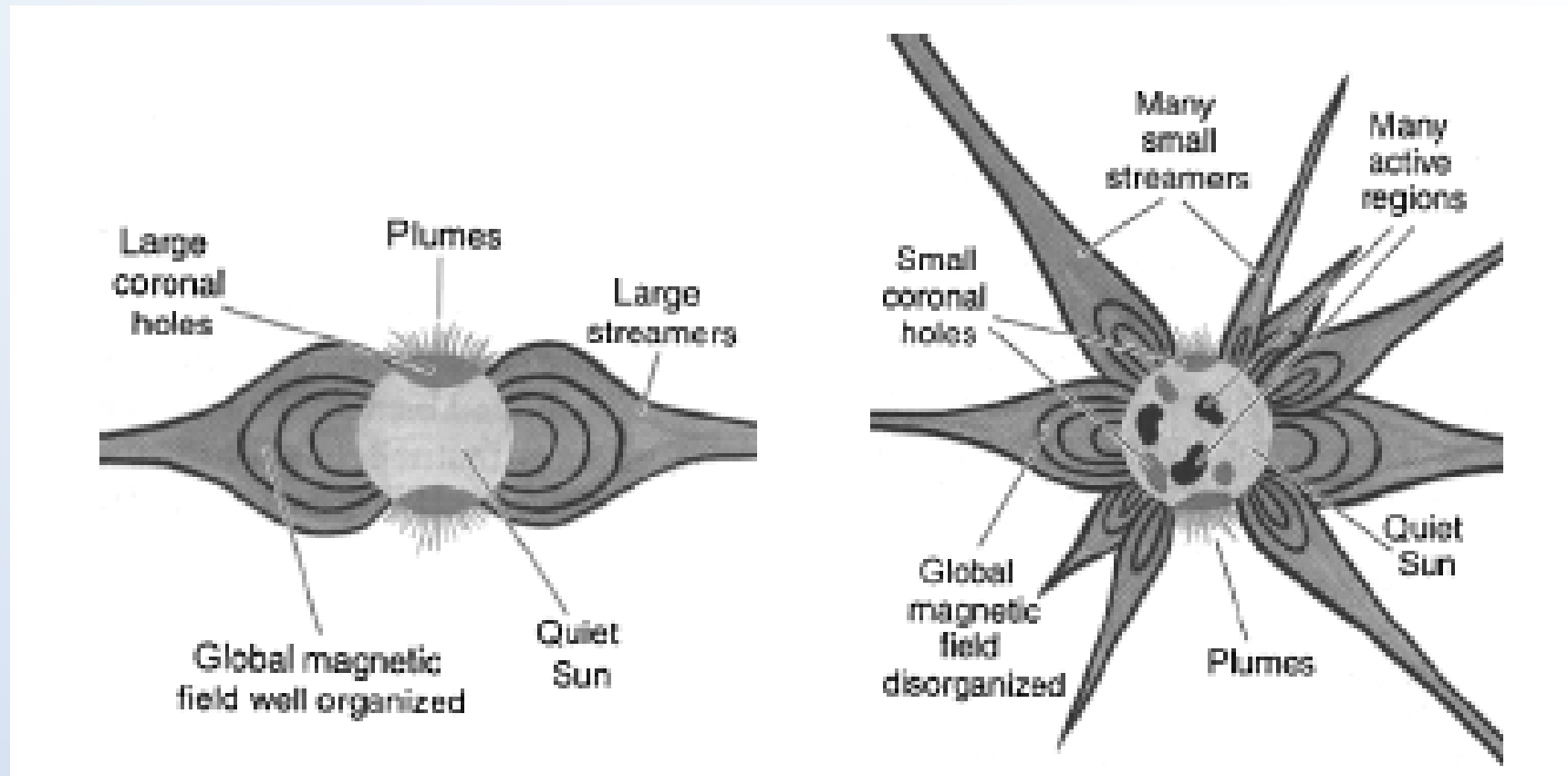
- Maps of the photosphere (top) and source surface ($2.5 R_s$) (bottom)
 - **red**: positive field,
blue: negative field
- Dotted line denotes the magnetic neutral line/HCS
- Horizontal line denotes the latitude of the Earth with color indicating HF polarity at 1 AU.



Corona over the solar cycle

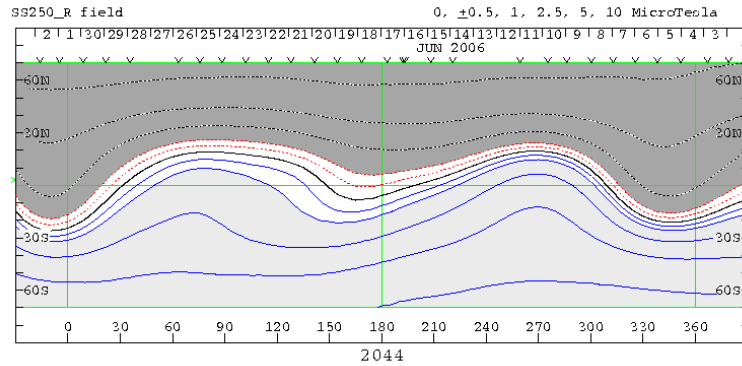
During **solar minimum times** coronal streamers are confined to the equatorial region, with coronal holes covering large regions around the poles.

During **solar maximum times**, coronal streamers are fairly evenly distributed over the whole solar surface.

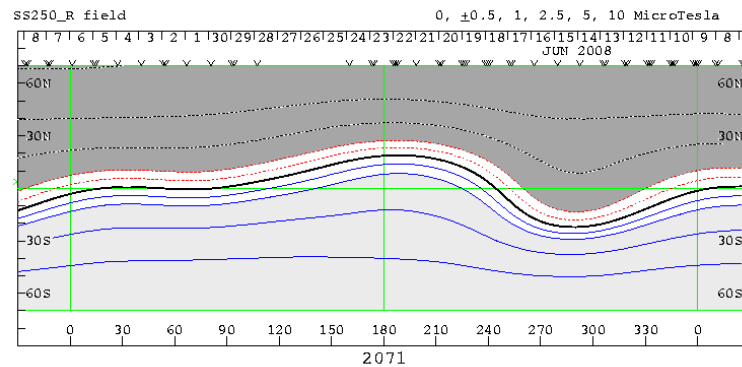


HCS over solar cycle synoptic latitude – longitude maps

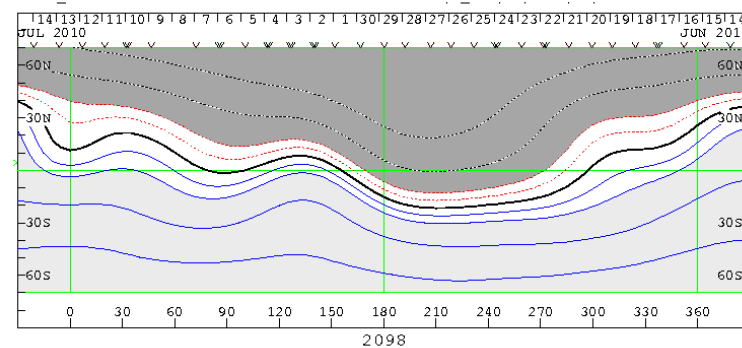
2006-06



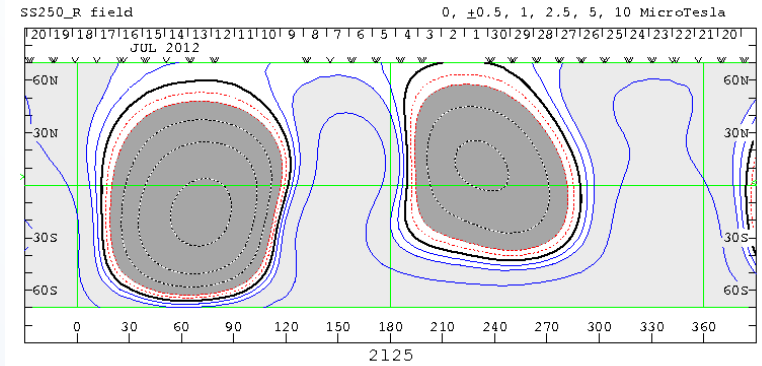
2008-06



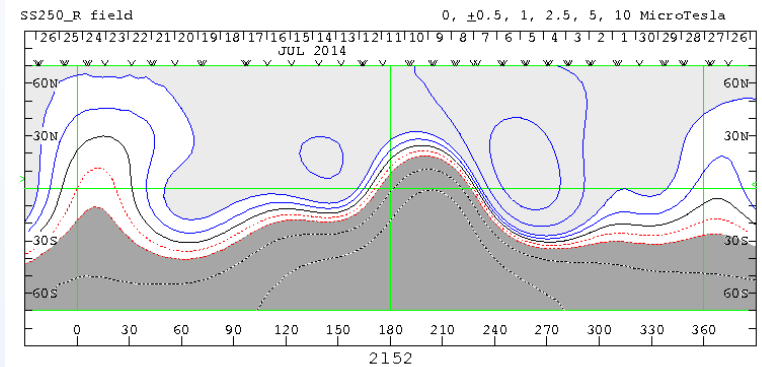
2010-06



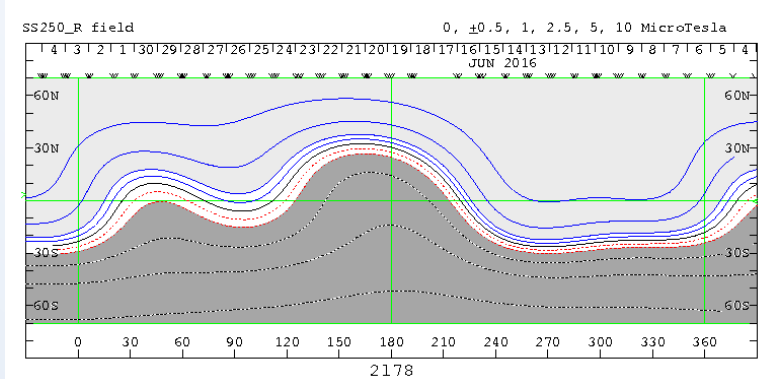
2012-06



2014-06

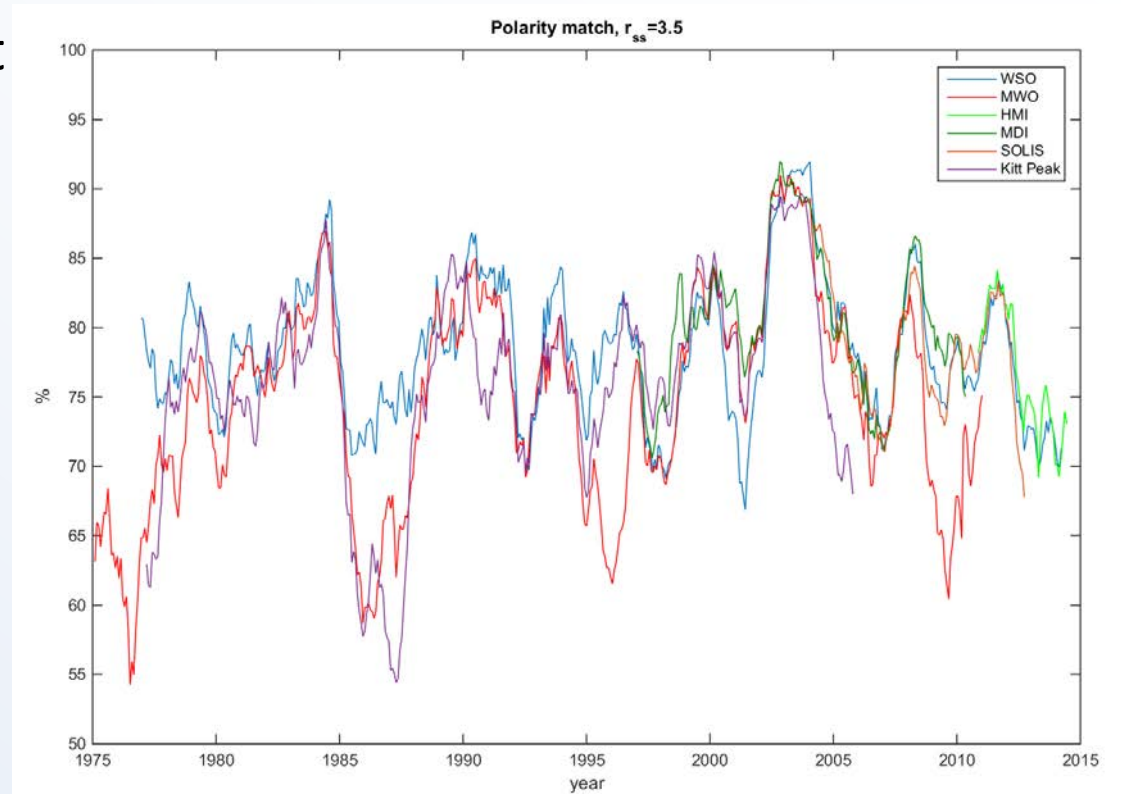


2016-06



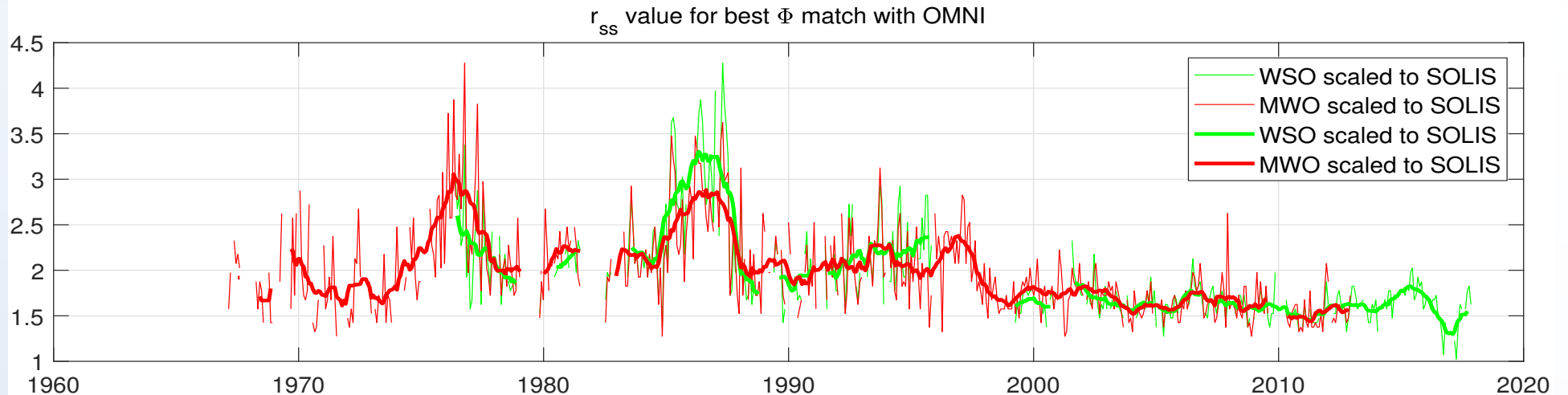
PFSS: Polarity comparison

- Polarity match between HMF at 1 AU and coronal field from six observatories.
- Polarity match varies between about 70% and 85%.
- Generally a **very good agreement** between all instruments.
- MWO and Kitt Peak data are slightly less successful, since they have some problems with polar fields.



J. Koskela, I. I. Virtanen, and K. Mursula, Comparing coronal and heliopheric magnetic fields over several solar cycles, *Astrophys. J.*, 835, 63, 2017.

Optimum r_{ss}



There is an overall declining trend in optimum r_{ss} .

Most clearly there is stepwise decline in opt- r_{ss} in the late 1990s.

Even thereafter, a weak declining trend in opt- r_{ss} in 2000s (2010s?)
MWO and WSO agree on these changes.

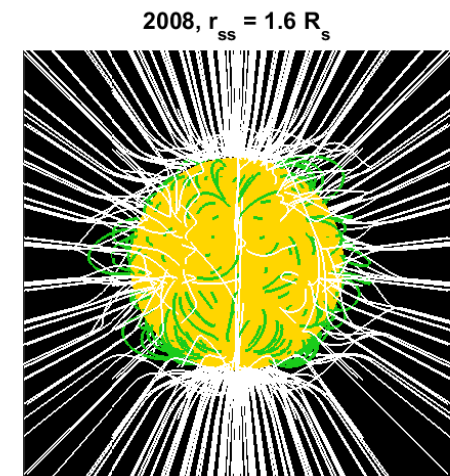
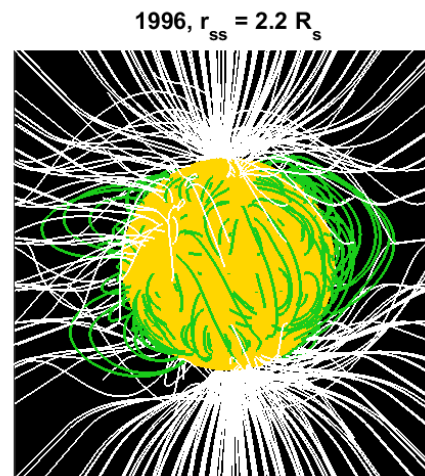
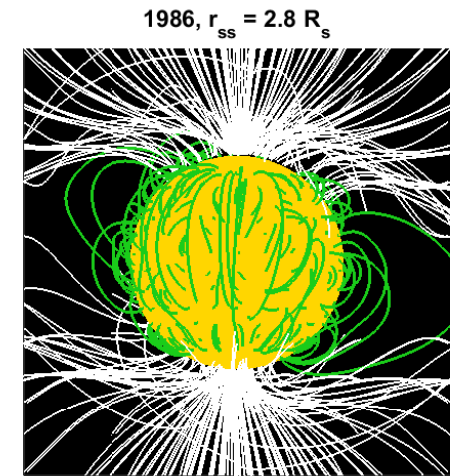
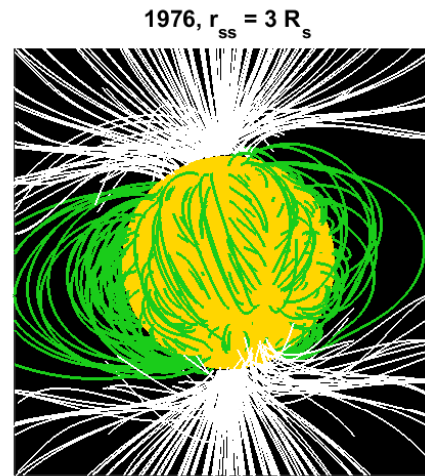
I. I. Virtanen, J. Koskela, and K. Mursula, Abrupt shrinking of solar corona in the late 1990s, *Astrophys. J. Lett.*, 889:L28, 2020.

Coronal field in 4 minima

In 1976, coronal closed fields were dominated by long **inter-hemispheric field lines**, reflecting strong polar fields and large r_{ss} distance.

In 2008, corona had mostly **intra-hemispheric field lines**, reflecting weaker polar fields and smaller r_{ss} distance.

I. I. Virtanen, J. Koskela, and K. Mursula, Abrupt shrinking of solar corona in the late 1990s, *Astrophys. J. Lett.*, 889:L28, 2020.



Solar wind

Solar wind: Comet tails

Ludwig Biermann, 1951: A part of comet tail points always **directly away from Sun**.

=> It must consist of ionized gas pushed away by solar ionized gas, the solar wind.

Towards the Sun



Image of comet Hale Bopp in 1997

Solar wind forms the **ion tail** of comets.

Solar wind must have a very high speed relative to the comet. Biermann estimated the solar wind speed to be about 500 km/s.

This was an astonishingly good estimate.

Radiation pressure on dust grains forms the diffuse **dust tail**.

Pressure pushes the grains away from Sun.

However, they **fall behind** the radial direction because their angular speed is lower than earlier, closer to the nucleus.

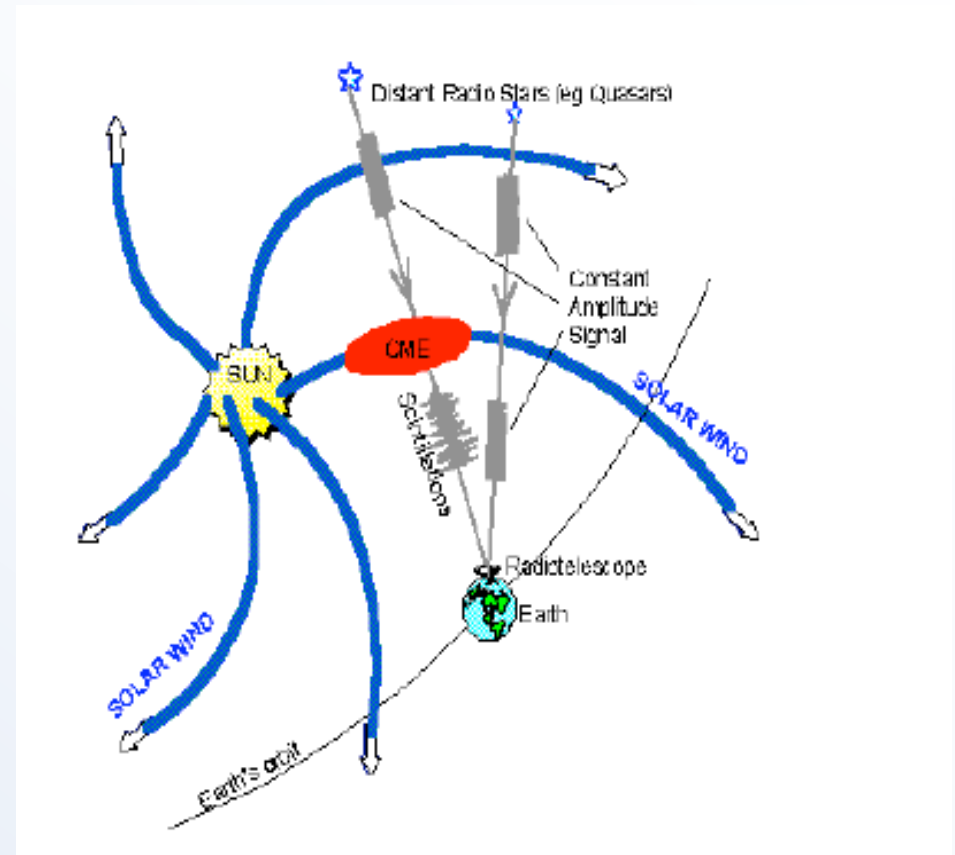
Therefore dust tails are curved from radial direction.

Interplanetary scintillation

Random fluctuations in the intensity, phase and polarization of radio waves of celestial origin.

When measuring radio waves, e.g., from distant radio galaxies, the **density variations of solar wind plasma** on the path of the radio waves can cause small disturbances (phase shifts, amplitudes changes), or **scintillations**, to the waves.

The closest **analogy** is the **twinkling** of stars and planets by the turbulence in the Earth's atmosphere caused by moving water vapor in the atmosphere.

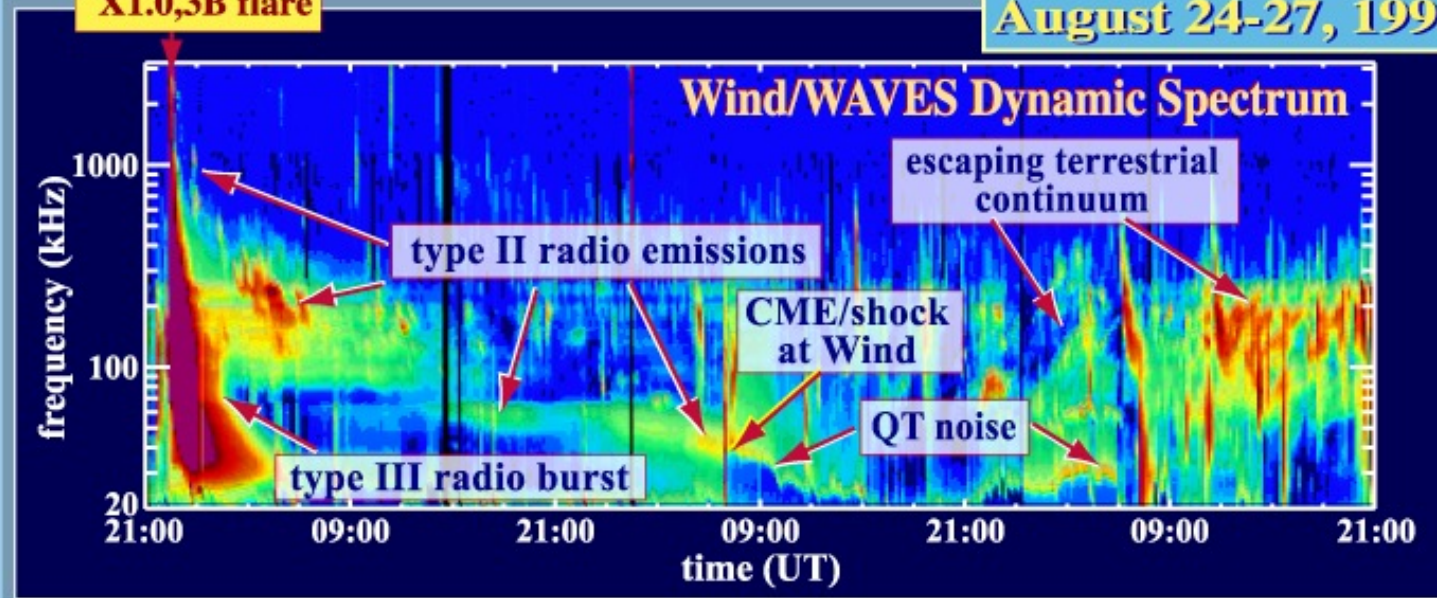


Radio waves

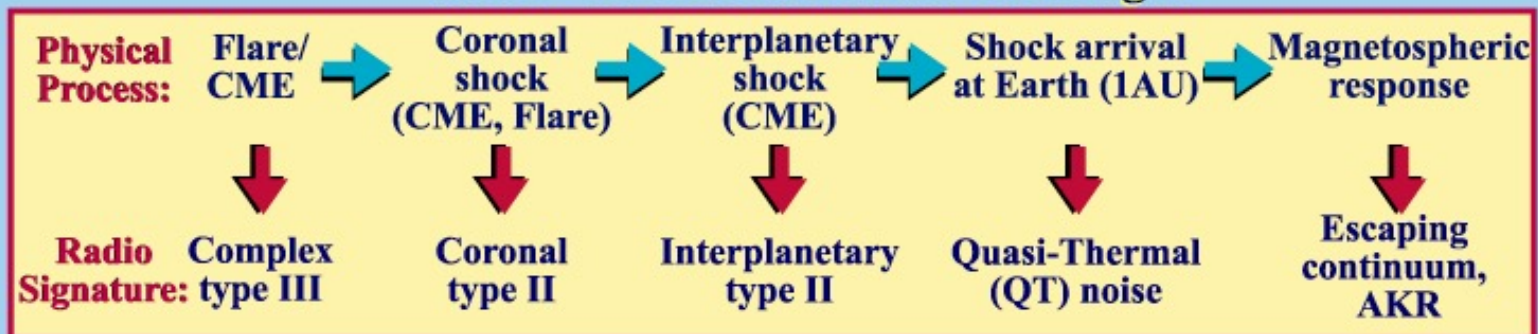
Radio Signatures of a Solar-Terrestrial Event

X1.0,3B flare

August 24-27, 1998



Solar - Terrestrial Radio Paradigm

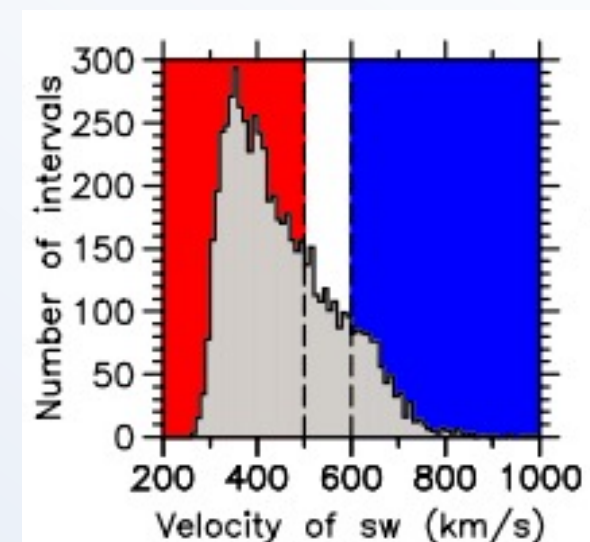
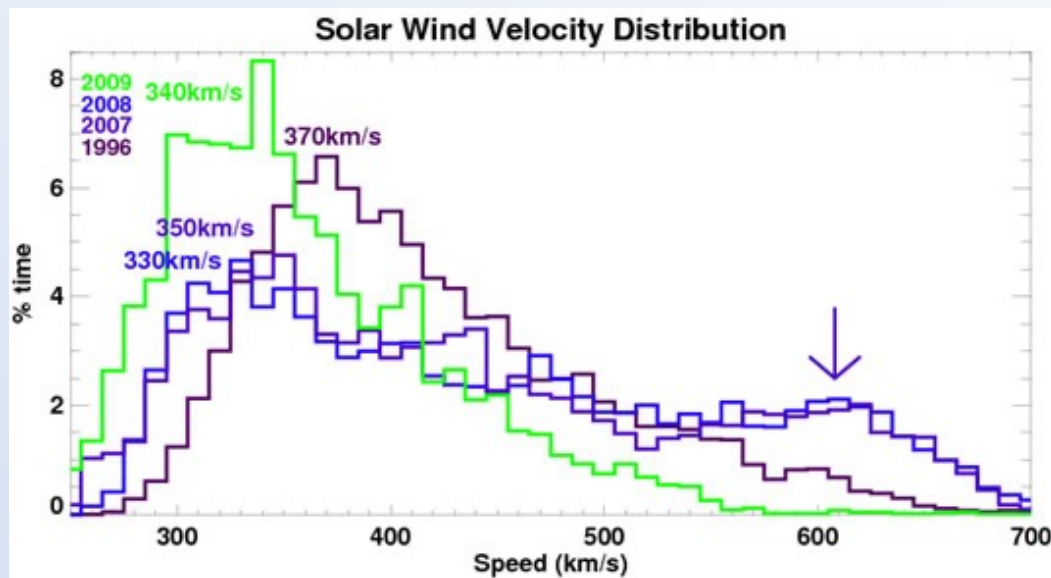


In-situ observations

- First satellite observations in early 1960s
- Continuous in-ecliptic observations of solar wind and heliospheric magnetic field since 1964.
- Deep space missions Voyager 1 and 2, Pioneer 10 and 11, and New Horizon.
- Ulysses observations of high heliographic latitude.
- Inner heliosphere missions like Helios-1 and 2, Solar Parker Probe, Solar Orbiter
- Future missions: L5/L4, SPORT (Chinese)...

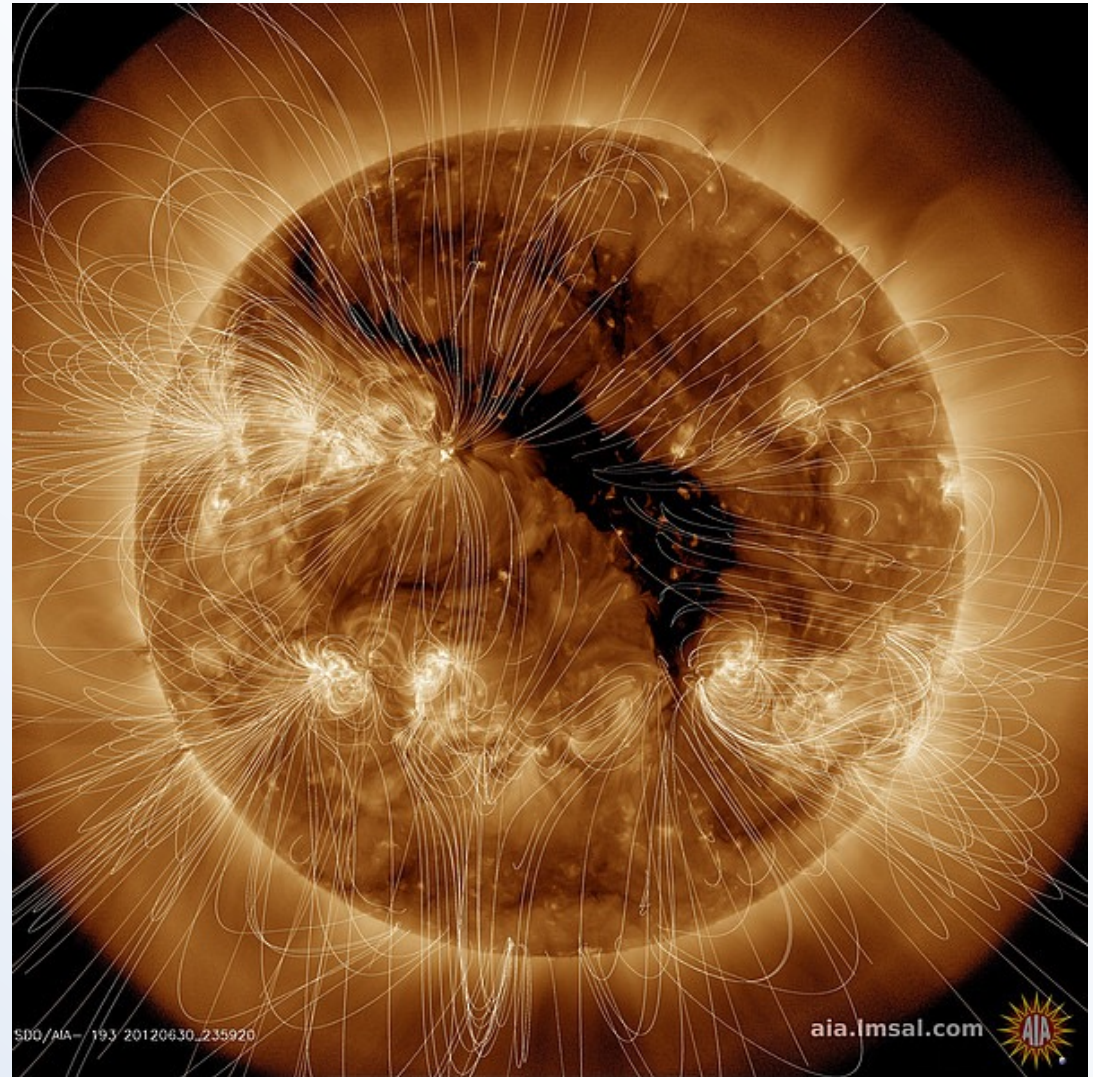
Solar wind velocity at Earth

- The average solar wind speed is 400-500 km/s
- Speed varies from 200km/s to 2000km/s, significant solar cycle variations
- The very highest velocities relate to Coronal Mass Ejections (CME).
- Large scale flow is radial (only small azimuthal and polar components)

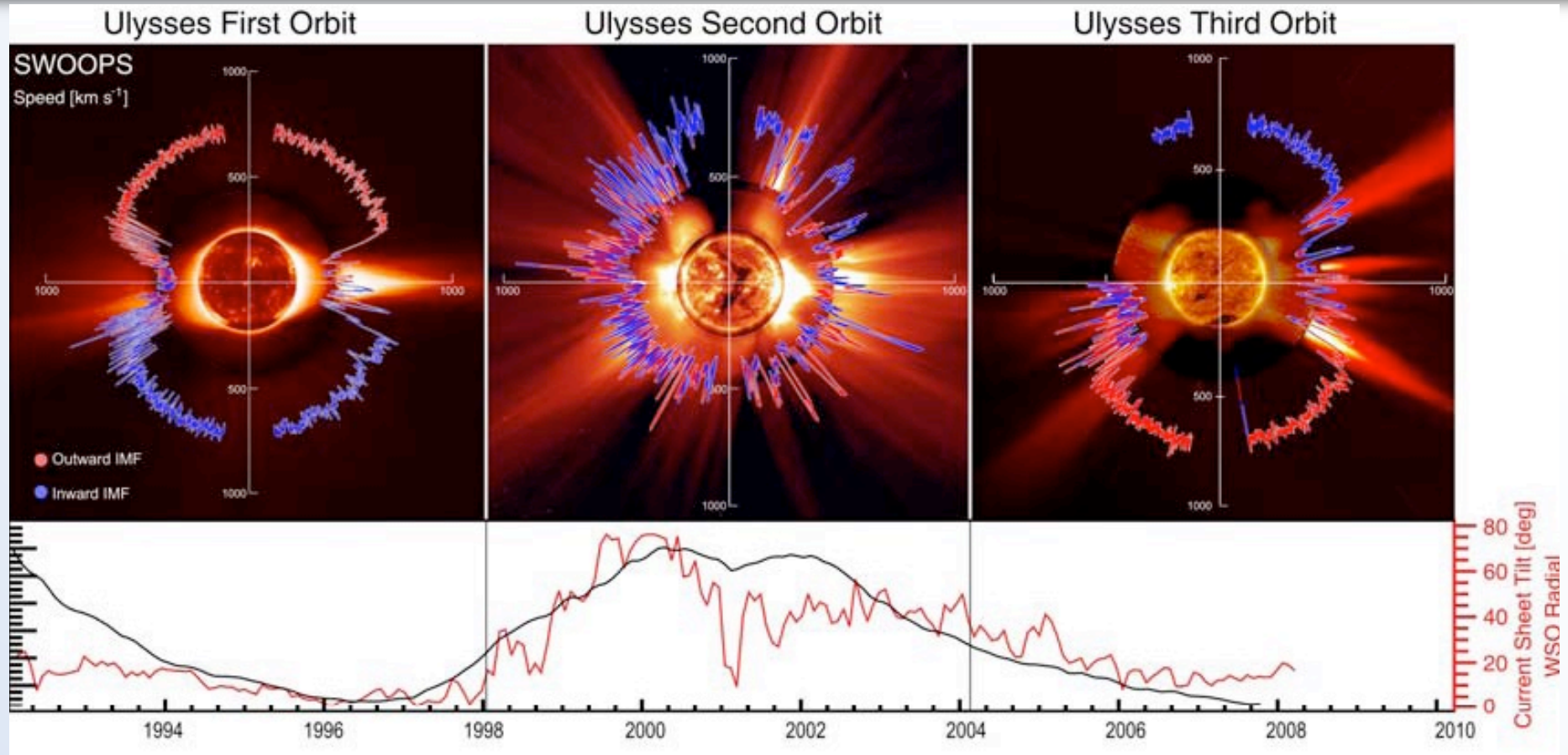


Fast and slow solar wind

- **Fast solar wind** originates from large coronal holes, where magnetic field is open
- **Slow solar wind** originates from streamers above active regions, and probably from small coronal holes and coronal hole boundaries, but the origin is **not exactly known yet!**

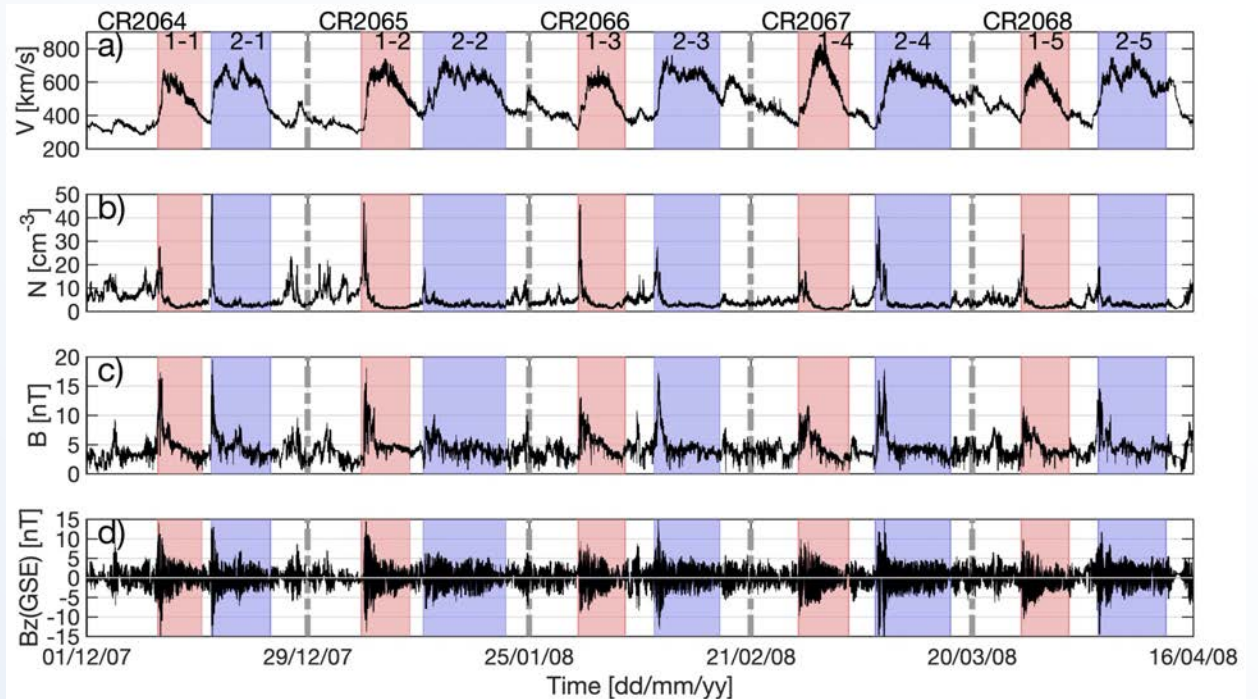
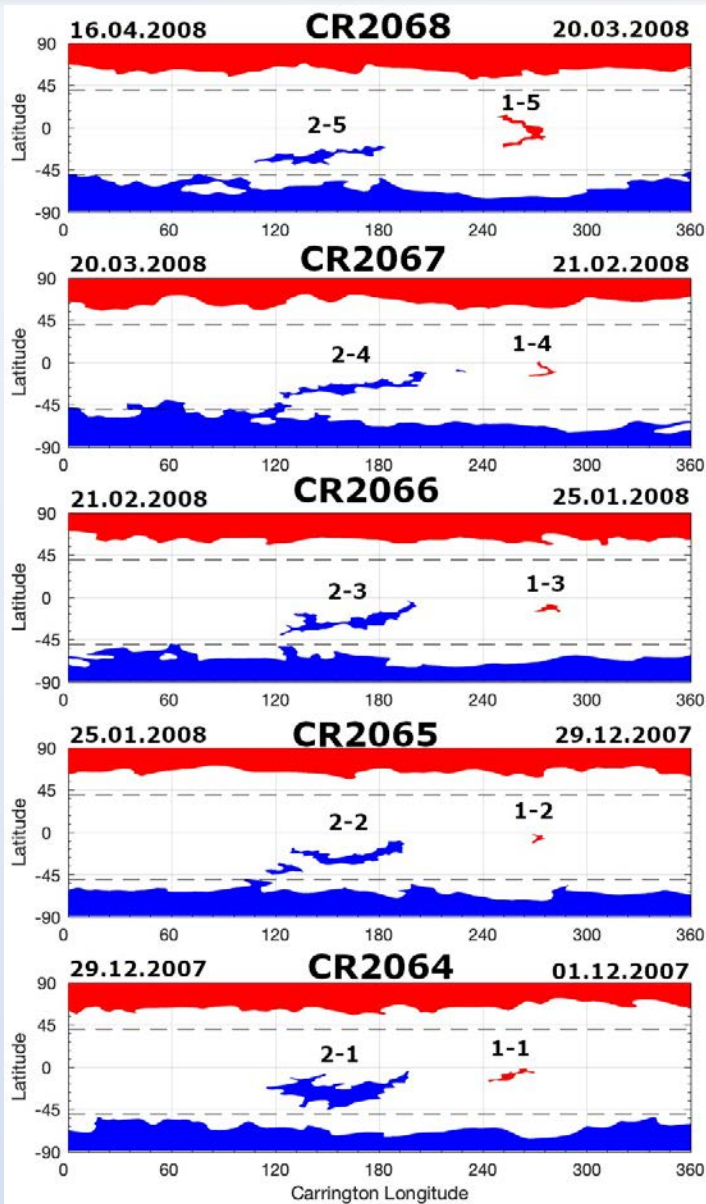


Ulysses results: 3D solar wind



- Ulysses found continuous fast solar wind (~ 750 km/s) at high latitudes at solar minimum in agreement with the idea that fast solar wind originated in coronal holes. This fast wind was associated with large stable polar coronal holes.
- Slow solar wind is associated with the streamers seen in coronagraph images.

Solar wind streams and coronal holes



Two HSSs with opposite magnetic polarities from equatorial coronal holes repeat during many solar rotations.

C. Munteanu, A. Hamada and K. Mursula, High-speed streams in 2007-2008: Turning on the Russell-McPherron effect, J. Geophys. Res.: Space, 124, 2019.

Fast and slow solar wind properties at Earth

Average solar wind parameters at 1 AU, for the time around solar activity minimum.

	Slow wind	Fast wind
Flow speed v_P	250–400 km s ⁻¹	400–800 km s ⁻¹
Proton density n_P	10.7 cm ⁻³	3.0 cm ⁻³
Proton flux density $n_P v_P$	3.7×10^8 cm ⁻² s ⁻¹	2.0×10^8 cm ⁻² s ⁻¹
Proton temperature T_P	3.4×10^4 K	2.3×10^5 K
Electron temperature T_e	1.3×10^5 K	1×10^5 K
Momentum flux density	2.12×10^8 dyn cm ⁻²	2.26×10^8 dyn cm ⁻²
Total energy flux density	1.55 erg cm ⁻² s ⁻¹	1.43 erg cm ⁻² s ⁻¹
Helium content	2.5%, variable	3.6%, stationary
Sources	Streamer belt	Coronal holes

- **Fast solar wind** from coronal holes is (fast), hot and not dense
- **Slow solar wind** from streamer belt is (slow), cold and dense

Coronal temperature and solar wind

- Large coronal holes are sources of fast solar wind and appear as dark regions in coronagraphs due to the **lower density**.
- Comparison of number densities of ion charge states shows that the sources of fast solar wind are also **cooler**:

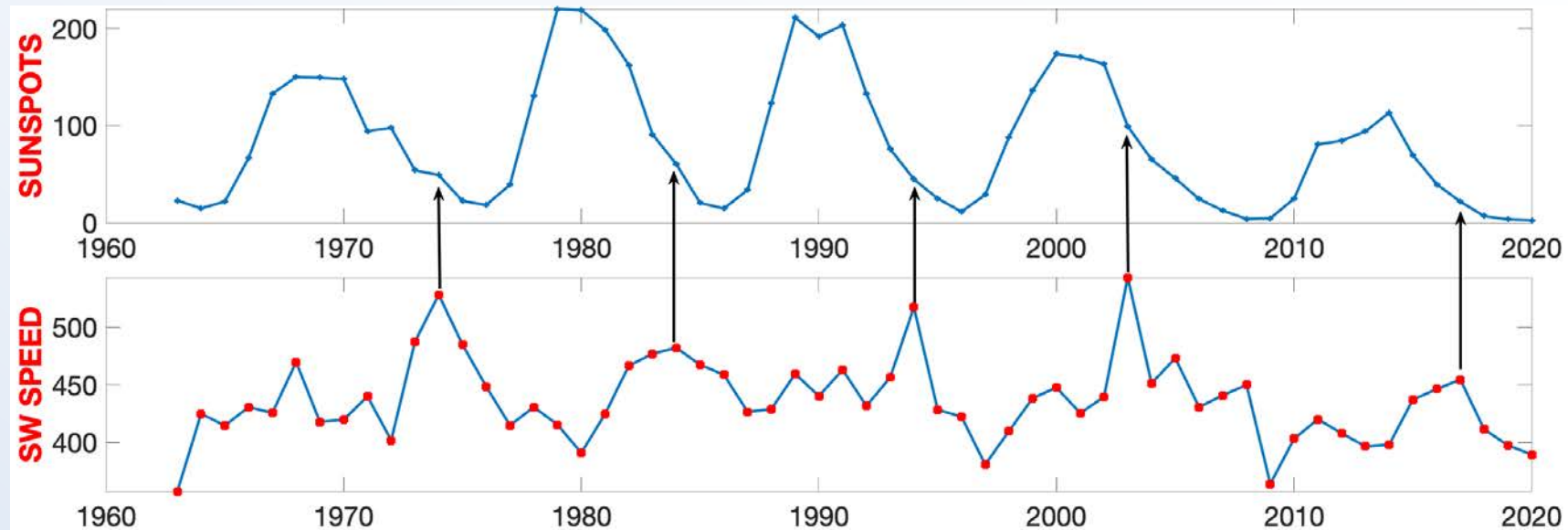
$$\frac{O^{7+}}{O^{6+}} \cdot \frac{C^{6+}}{C^{5+}} \left\{ \begin{array}{l} < 0.01 \rightarrow \text{coronal hole plasma} \\ > 0.01 \rightarrow \text{plasma from other source} \end{array} \right\}$$

- Ion charge states are fixed at a critical temperature (altitude), where **expansion rate exceeds collision rate**.
- This temperature is called the **freezing-in-temperature**. Beyond that, the charge states remain the same.
- **NOTE, however, that the fast solar wind at 1 AU is hot!**

CIR/SIR

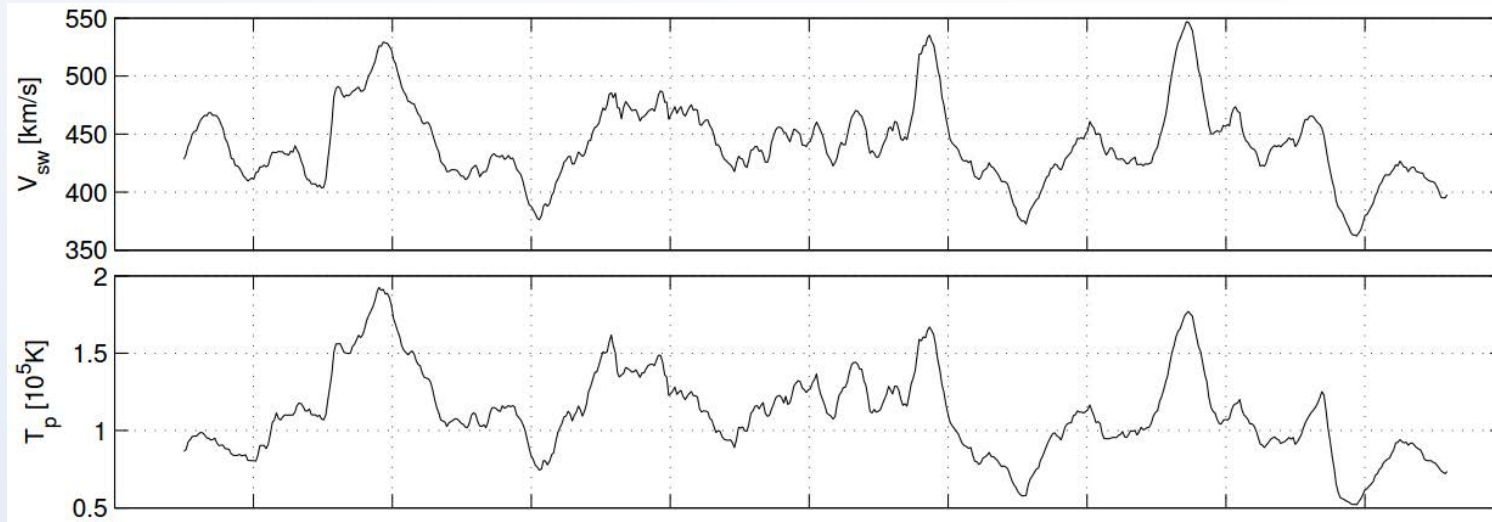
- The evolution of a high-speed solar wind stream (HSS), as it moves outward in the interplanetary space, produces **a stream interaction region (SIR)** with the background slow solar wind.
 - The two different plasma regions (flows or streams) are prevented from mixing due to the frozen-in magnetic fields.
- Because the HSS originates from a coronal hole which typically **persists** over several solar rotations, the HSS and the interaction region **repeat** several times at the solar rotation period interval
=> corotating (better: repeating) interaction region (**CIR**).

Solar cycle variability of SW speed



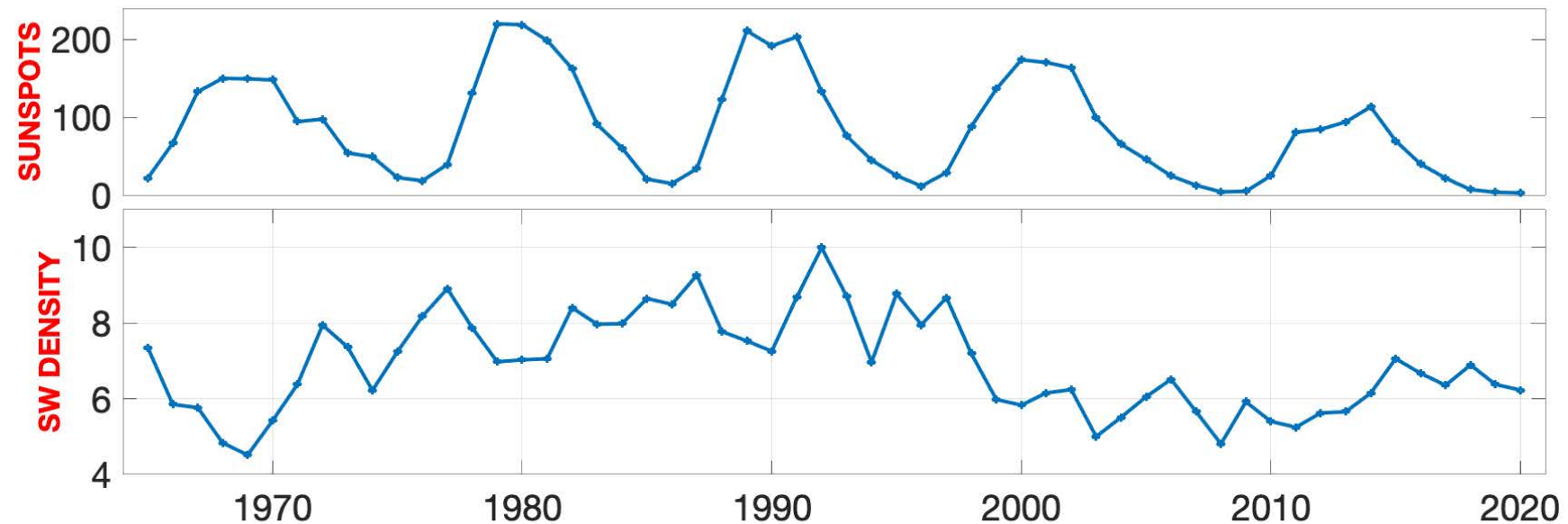
- SW velocity (measured at Earth; lower panel) reaches maximum in the **declining phase** of the solar cycle.
- This relates to the **solar cycle evolution of coronal holes**

Solar cycle variability of SW temperature



- SW speed (upper panel) and SW temperature (lower panel) vary **very similarly** and reach maxima in the **declining phase** of the solar cycle.

Long-term variation of SW density



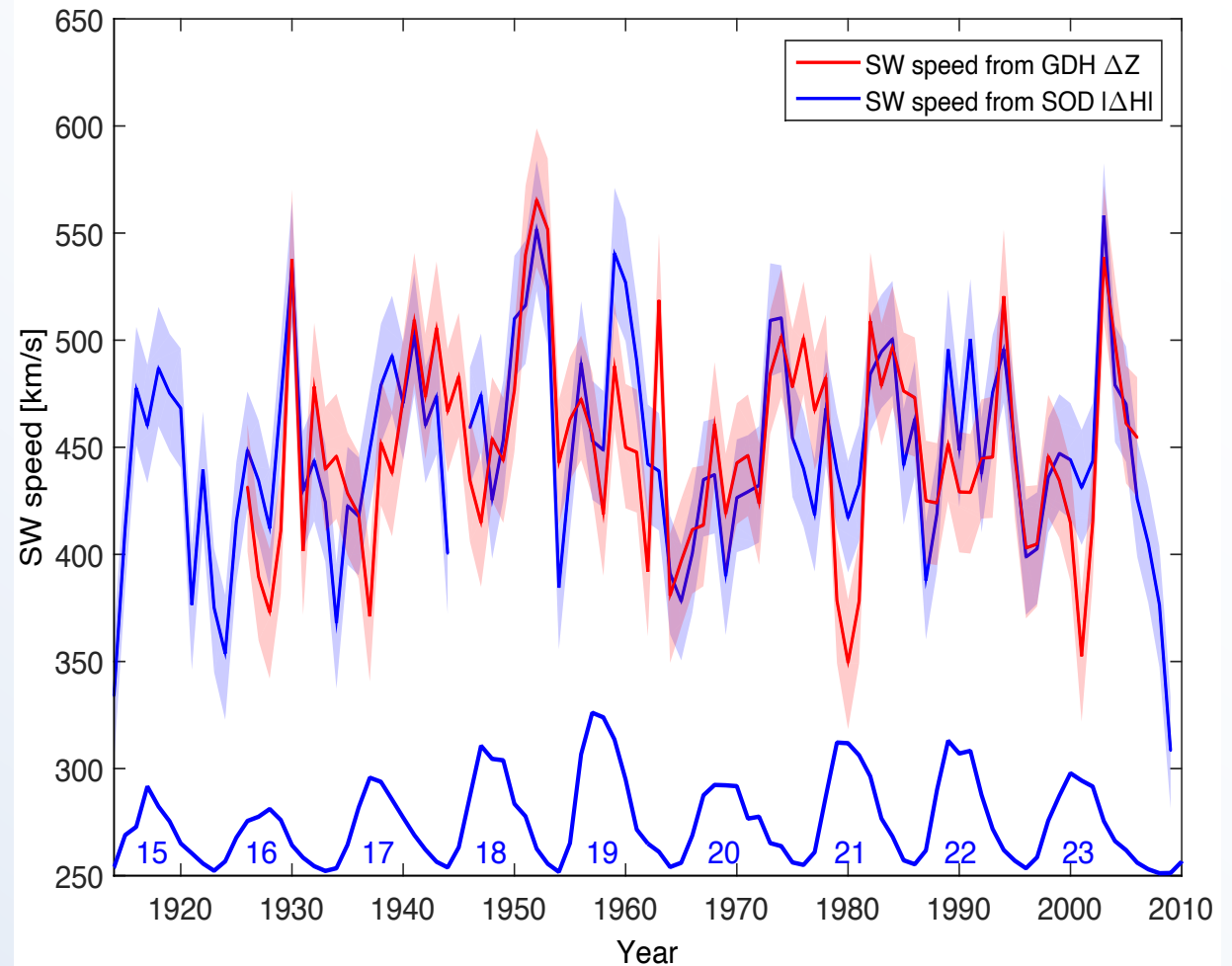
- SW density (measured at Earth; lower panel) does not show a clear cyclic evolution, but a **decreasing trend** since the late 1990s.

HSS/CIRs for the last century

Yearly mean solar wind speeds since 1914 obtained from geomagnetic activity.

Highest number of HSSs were found during **solar cycle 18**, just before the highest sunspot cycle 19.

This proves the **validity of the solar dynamo (Ω -effect)**, for the first time for this most dramatic period of solar activity.



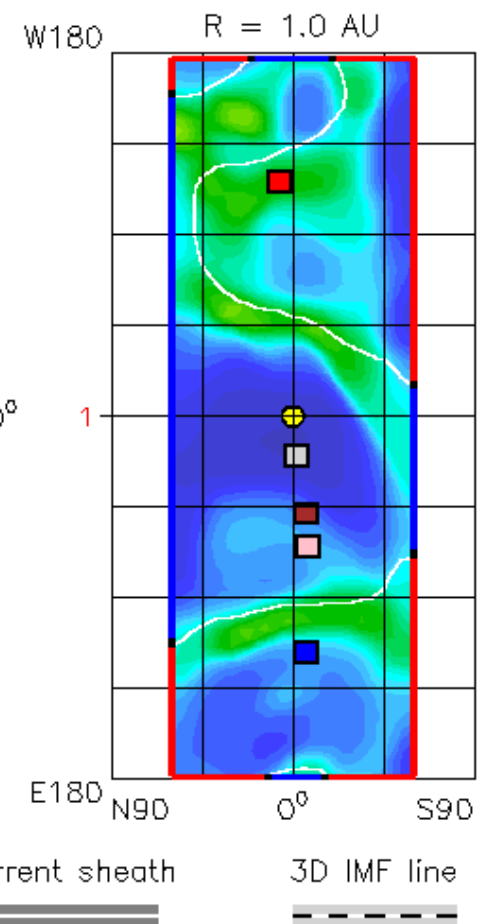
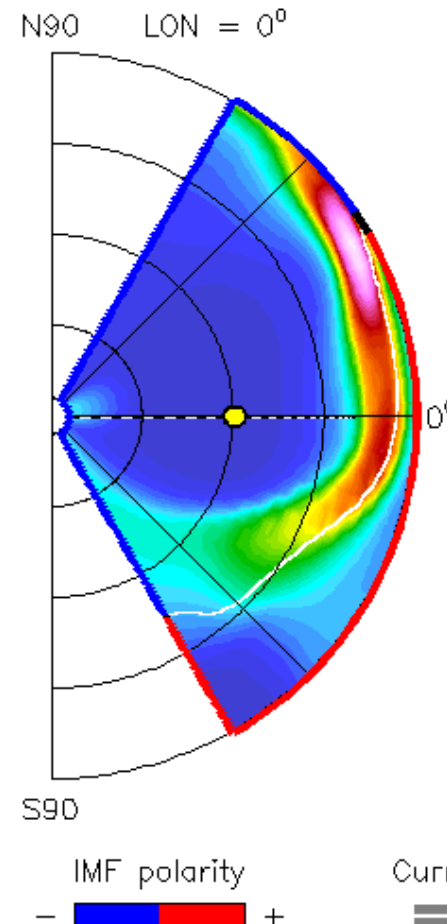
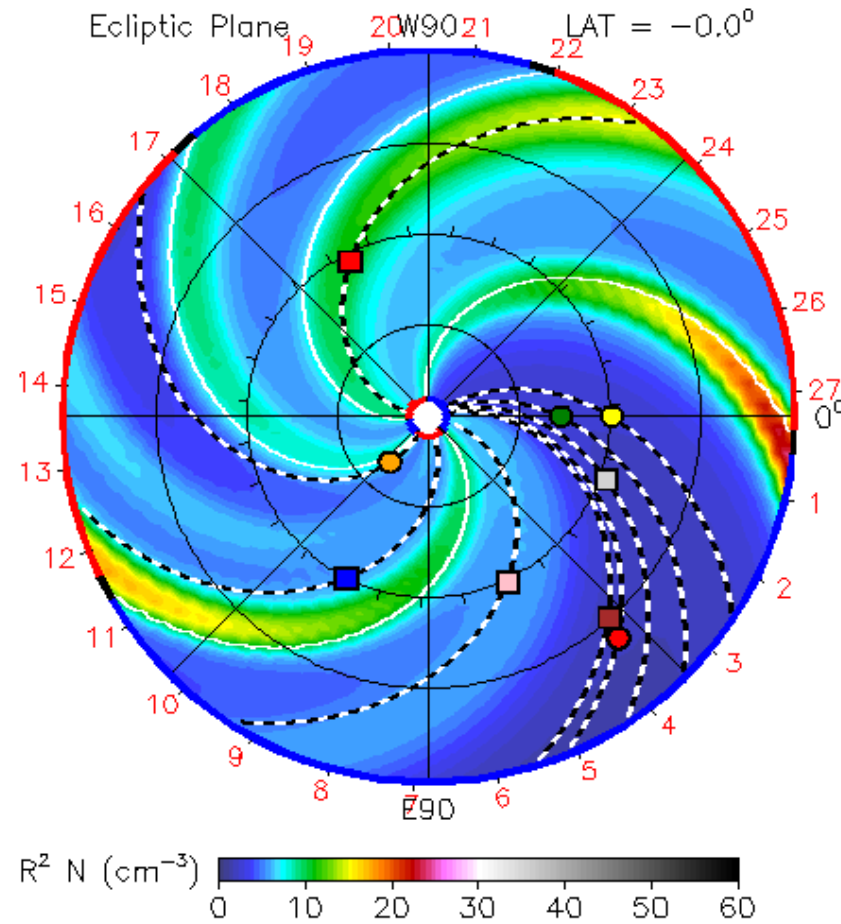
K. Mursula, R. Lukianova, and L. Holappa, Occurrence of high-speed solar wind streams over the Grand Modern Maximum, *Astrophys. J.*, 801, 30, 2015.

Solar wind and space weather models

2012-06-06T00:00

2012-06-06T00 +0.00 day

- Earth ● Mars ● Mercury ● Venus □ Kepler ■ MSL □ Spitzer ■ Stereo_A
- Stereo_B



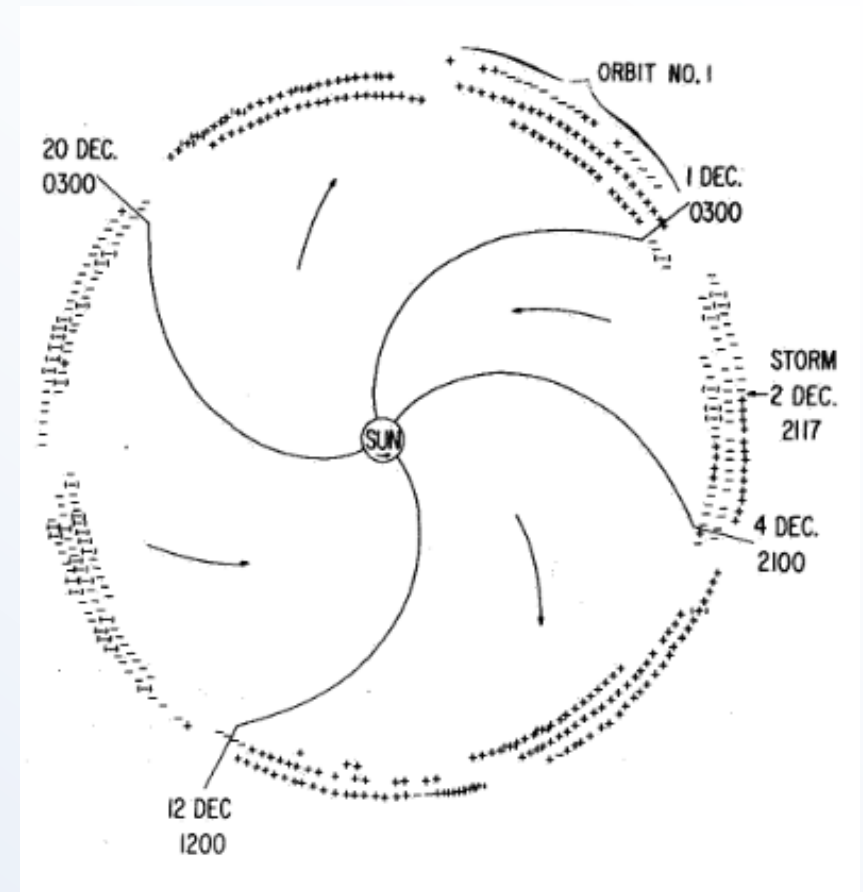
ENUL-2.7 lowres-2124-a3b1f WSA_V2.2 GONG-2124

cone/wsafr-cld/256x30x30x1.2124-a3b1f.16-mcp1umn1ed-1.053q5d2.gong-2012-06-06T00-2012-06-07

(Interplanetary magnetic field)
Heliospheric magnetic field

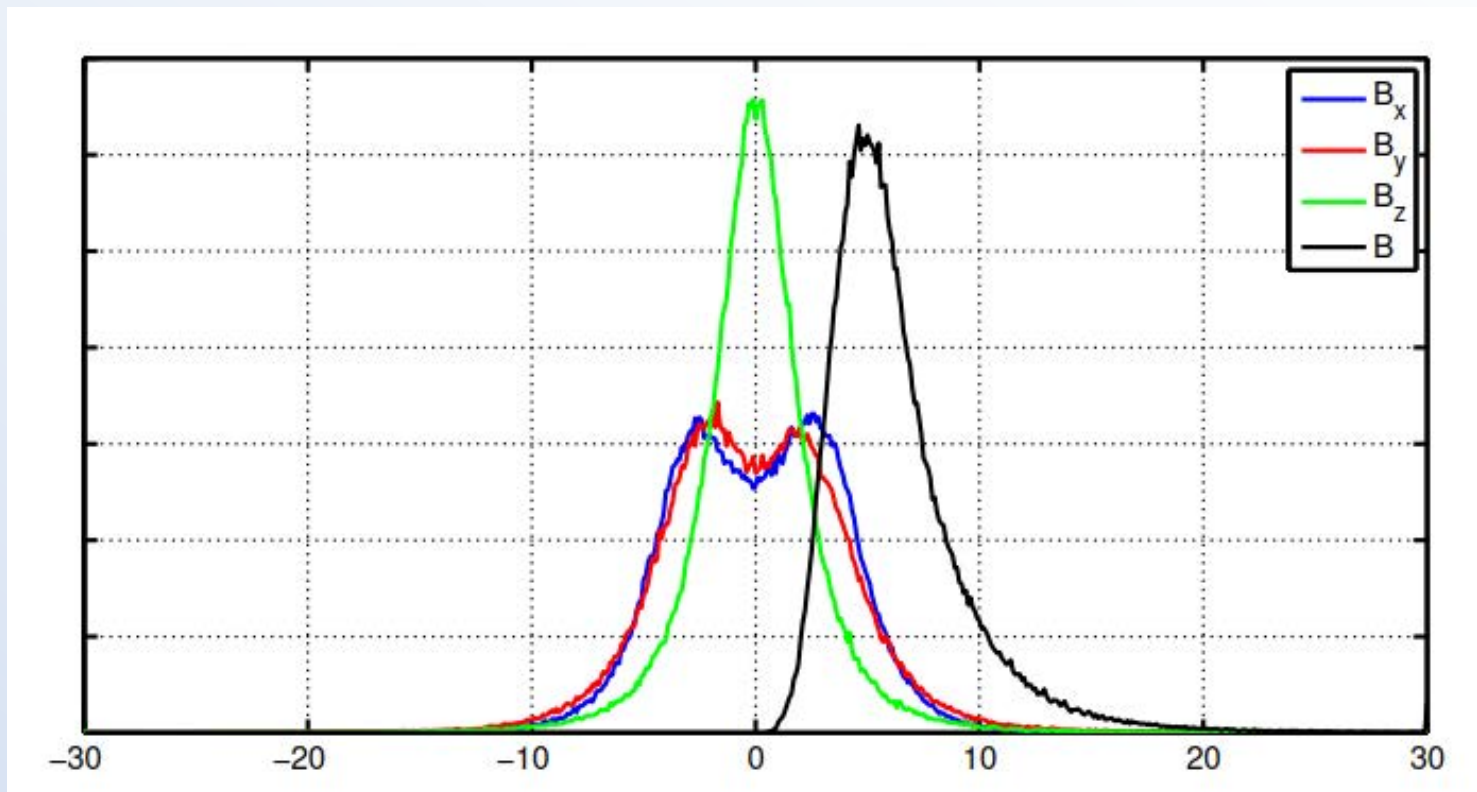
First observations of HMF

- IMP 1 satellite observations in 1963
- Magnetic field was found to have a **sector structure**, which is quite stable over a few rotations.
- Sector repetition period was found to correspond to solar rotation period.
- **Heliospheric magnetic field originates from the Sun!**
- HMF consist of sectors of **positive** ($B_r > 0$, Away-sector) and **negative** ($B_r < 0$, Toward-sector) **polarity** magnetic field.

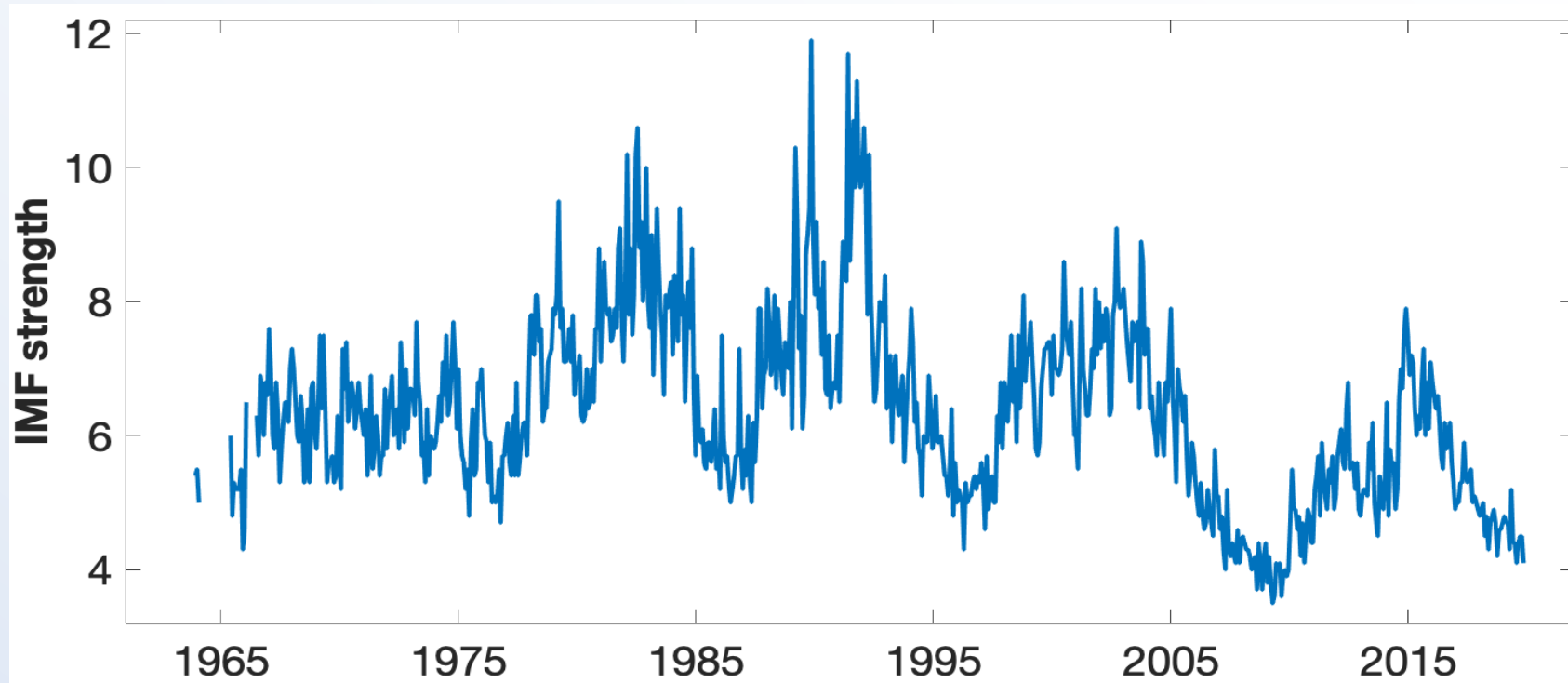


HMF distribution

- Distribution of 1h averaged HMF components observed at 1AU (GSE coordinate system).
- B_x and B_y depict **double peak** structure, corresponding to Toward and Away –sectors.



Long-term HMF strength at 1AU

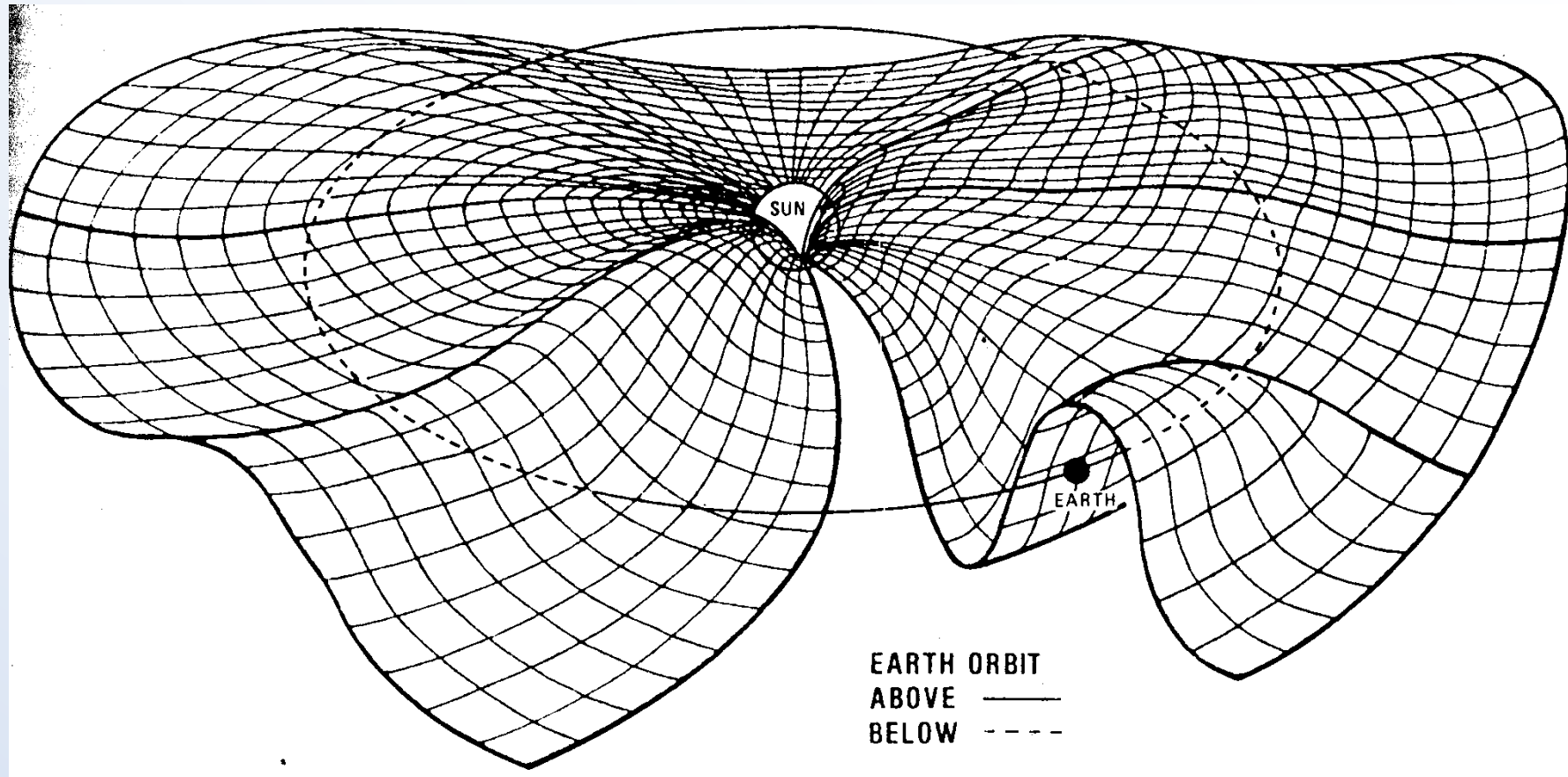


HMF strength depicts a **cyclic variation**, except during SC20.
A clear **declining trend** since 1990, reflecting the similar decrease of polar (coronal hole) fields.

Heliospheric current sheet

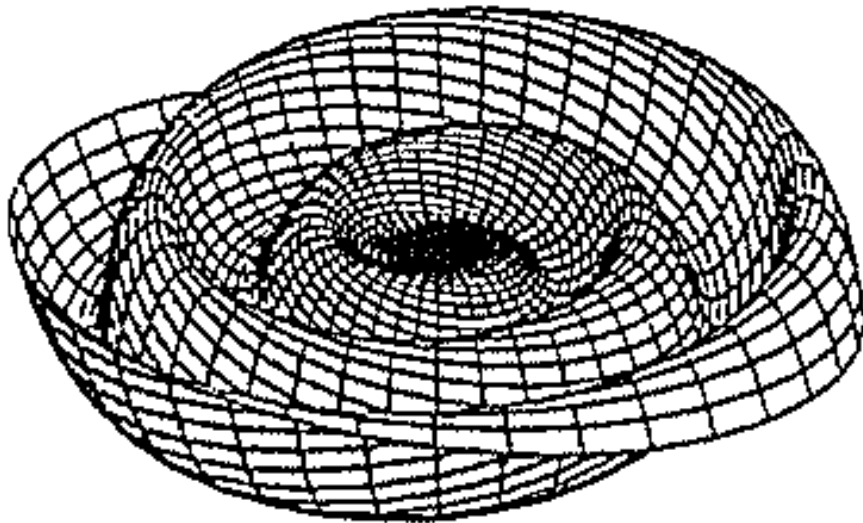
- **Heliospheric current sheet (HCS)** is a layer between the two opposite polarity sectors (including an **electric current**; more about that later).
- HCS is the extension of the **solar magnetic equator** to the heliosphere.
- During solar **minimum** times HCS is rather flat and mainly follows the solar equator.
- Tilted solar magnetic field leads to a **wavy HCS**.
- During the **declining** phase of solar cycle the HCS is quite flat and **tilted** with respect to the solar equator.
- During solar **maximum** times HCS configuration is complicated, and there can be **multiple** current sheets.

HCS = Ballerina skirt

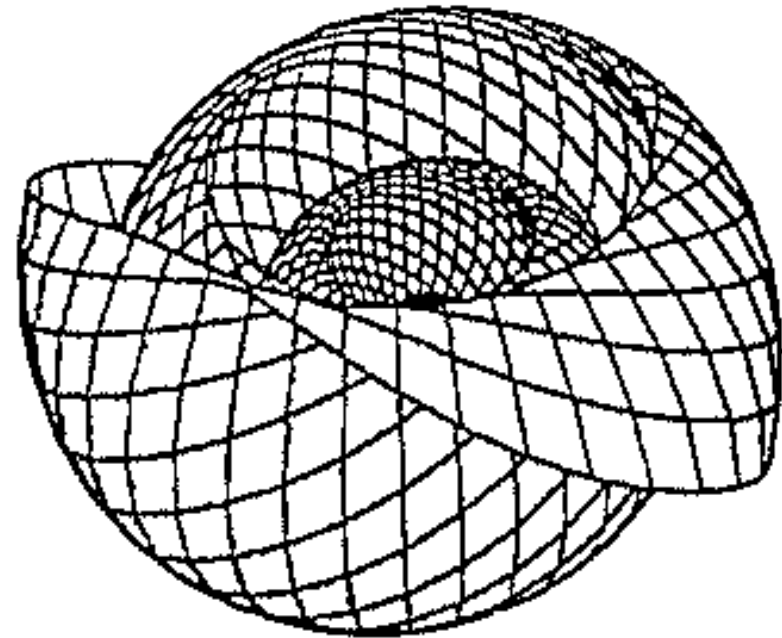


Heliospheric current sheet

Solar Minimum

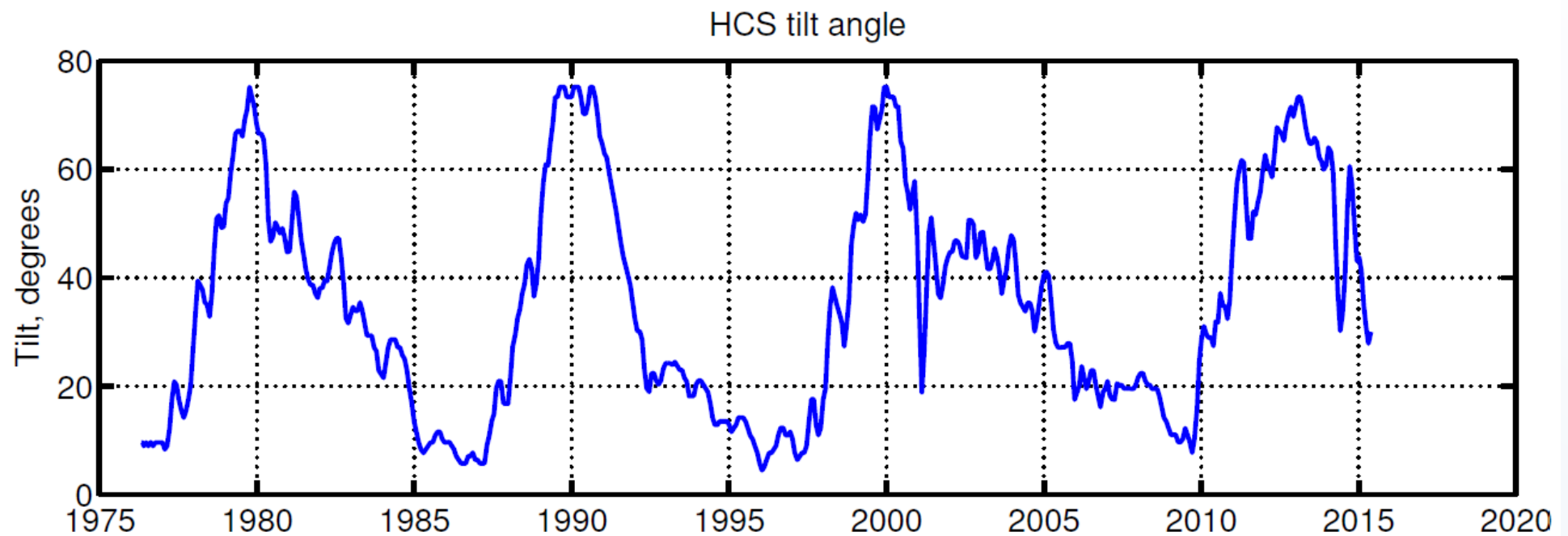


Solar Maximum



HCS tilt angle

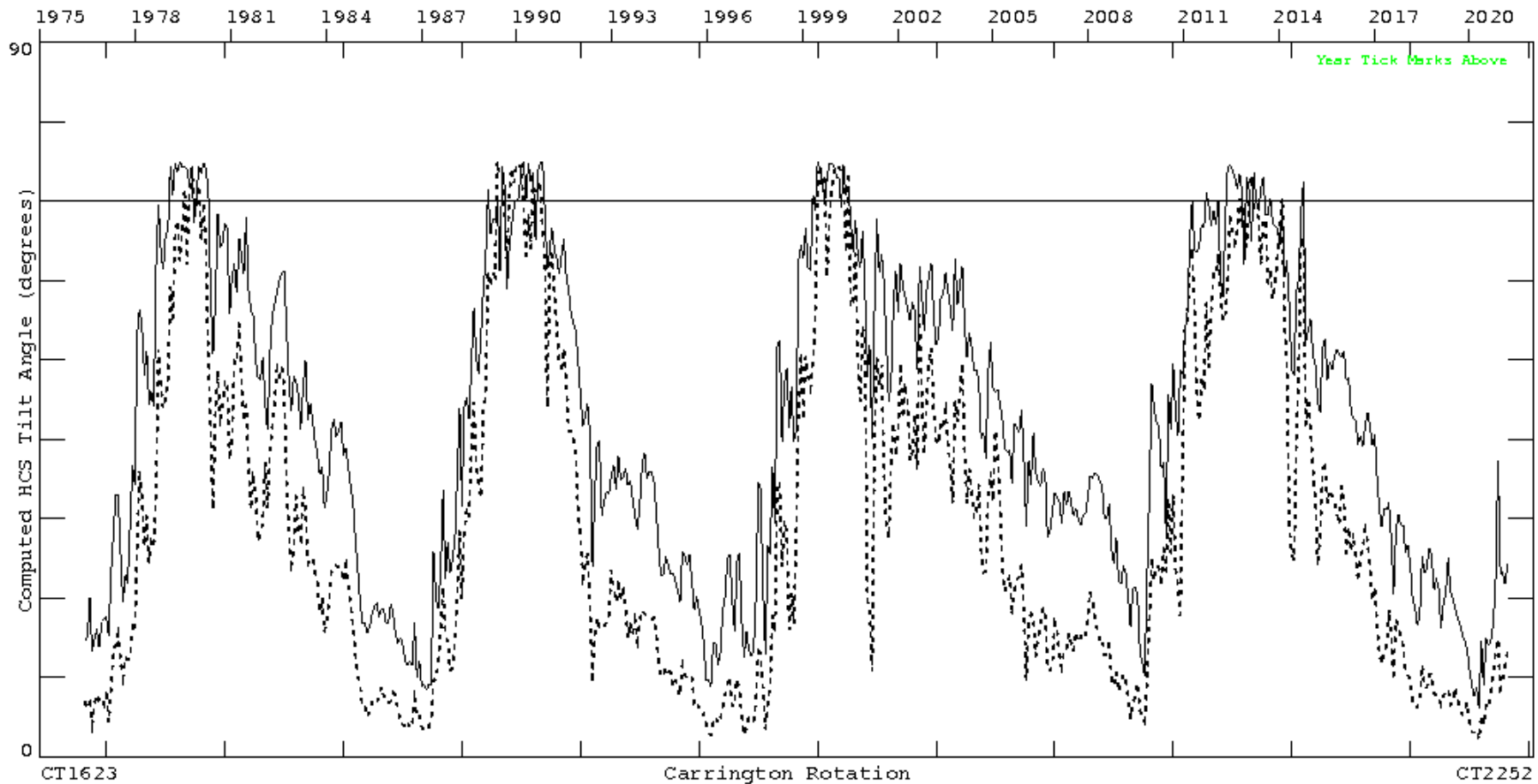
- Maximum latitudinal extent of the HCS
- Derived from PFSS model results
- One of the key parameters in cosmic ray models



HCS tilt angle

2021:04:28

Maximum Inclination of the Current Sheet (N-S Mean) : 1975-2021

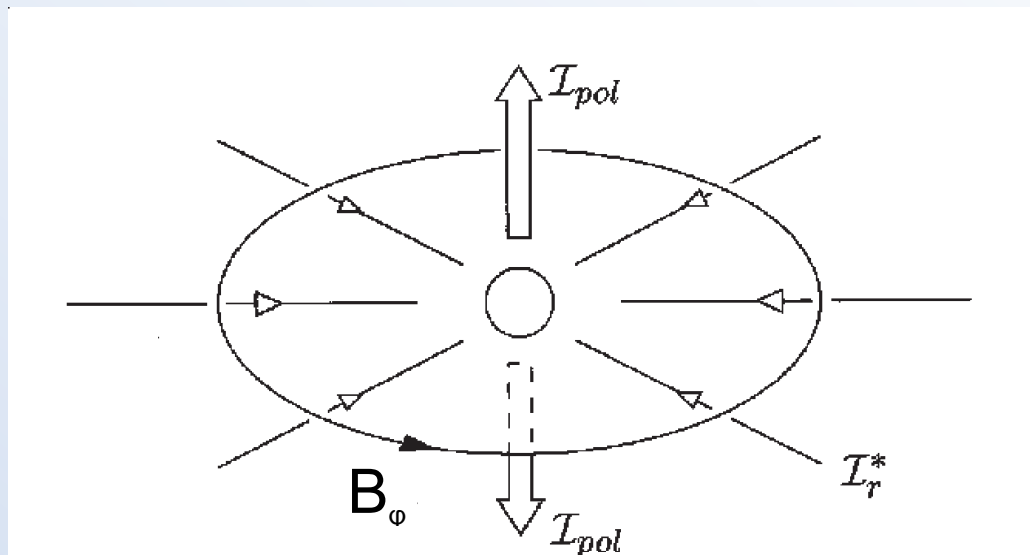


Solid=Classic PFSS Model (preferred)

Dashed=Radial $R_s=3.25$

HCS current

- **Oppositely directed** HMF fields can be close to each other around the HCS.
- **An electric current must flow in HCS** separating the oppositely directed magnetic fields.
- HCS is therefore called the **current sheet** (also the neutral sheet).
- The electric currents **originate** outside solar corona **in the interplanetary space**.
- **The currents reverse according to the overall polarity reversal from one cycle to another.**

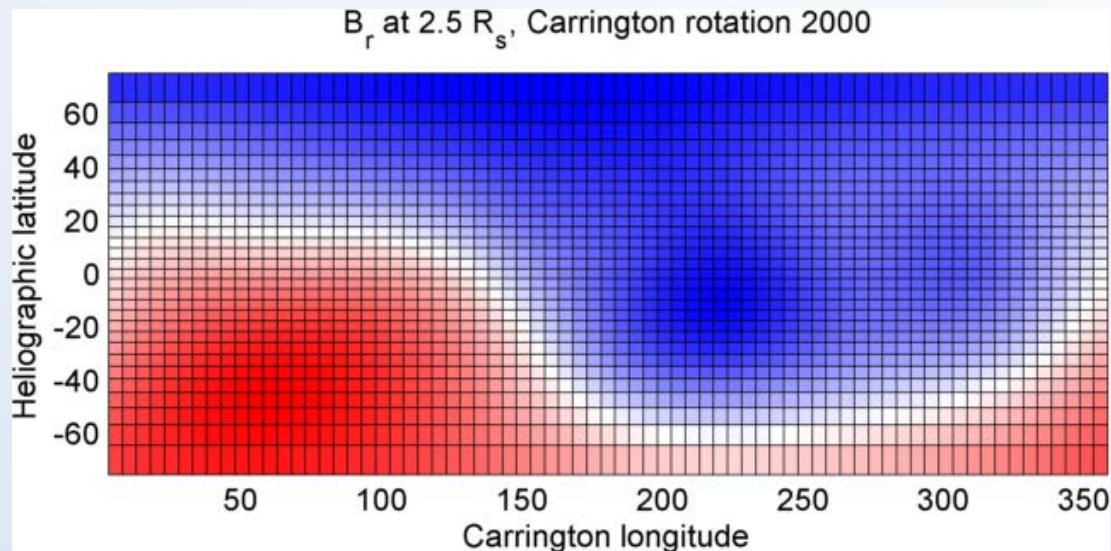


HCS latitude

The areas (solid angles Ω_+ and Ω_-) in solar corona covered by positive and negative polarities determine the rotationally averaged **heliomagnetic latitude (shift)** λ_m of the HCS:

$$\lambda_m = \sin^{-1} \left(1 - \frac{\Omega_+}{2\pi} \right)$$

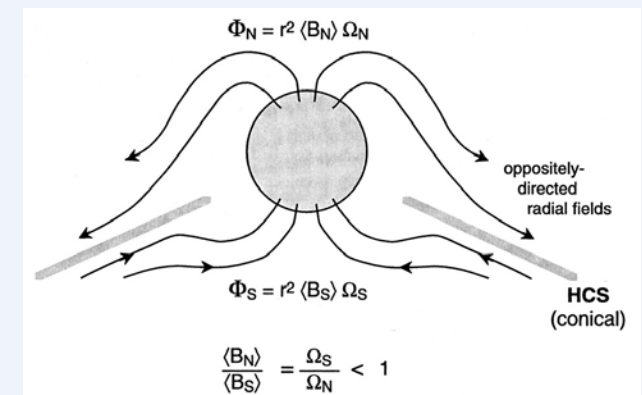
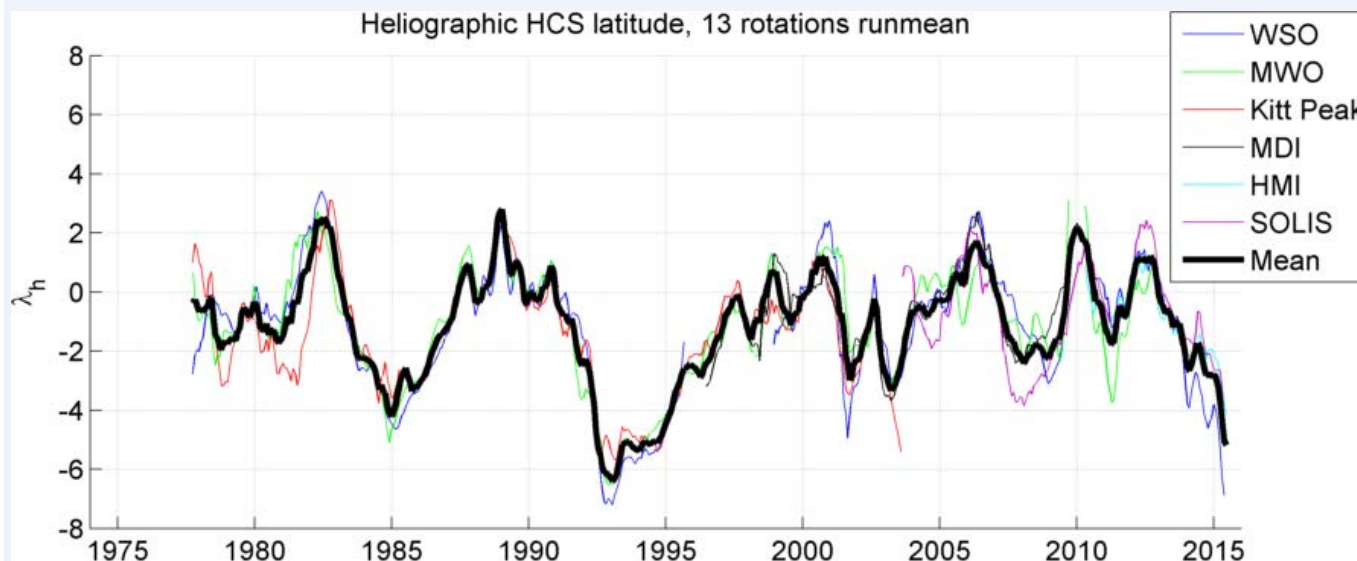
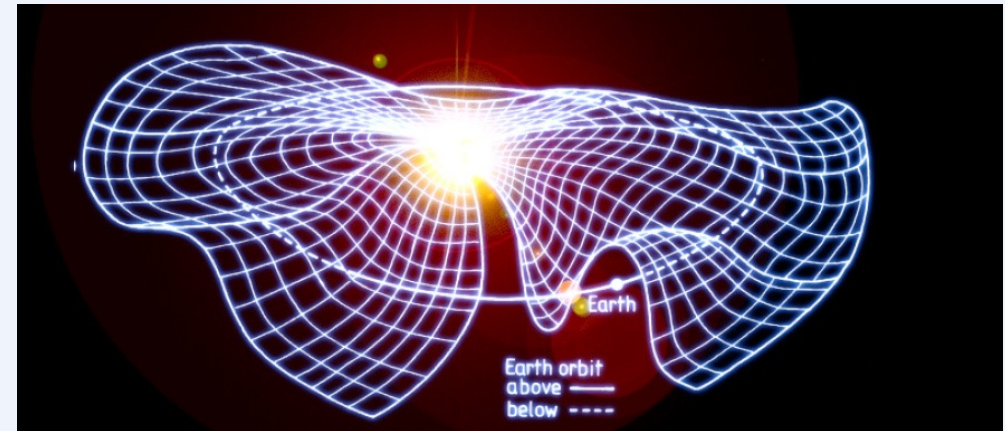
Heliographic latitude (shift) $\lambda_h = \lambda_m * \cos(\text{tilt angle})$



HCS = Heliospheric current sheet = Solar magnetic equator in space

HCS is southward shifted or coned by about 2 degrees during 3 years in the declining phase of solar cycle: **Bashful ballerina**

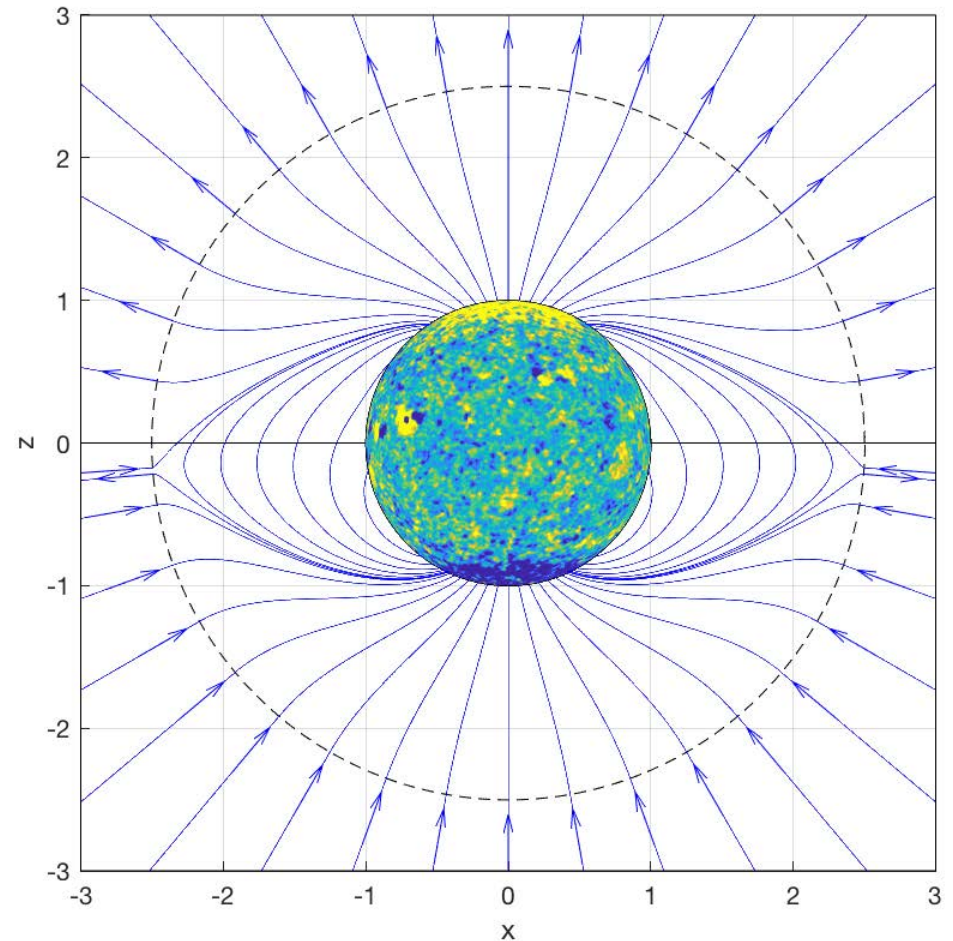
I. I. Virtanen, and K. Mursula, Photospheric and coronal magnetic fields in six magnetographs: I. Consistent evolution of the bashful ballerina, *Astron. Astrophys.*, 591, A78, 2016.



Coronal field asymmetry

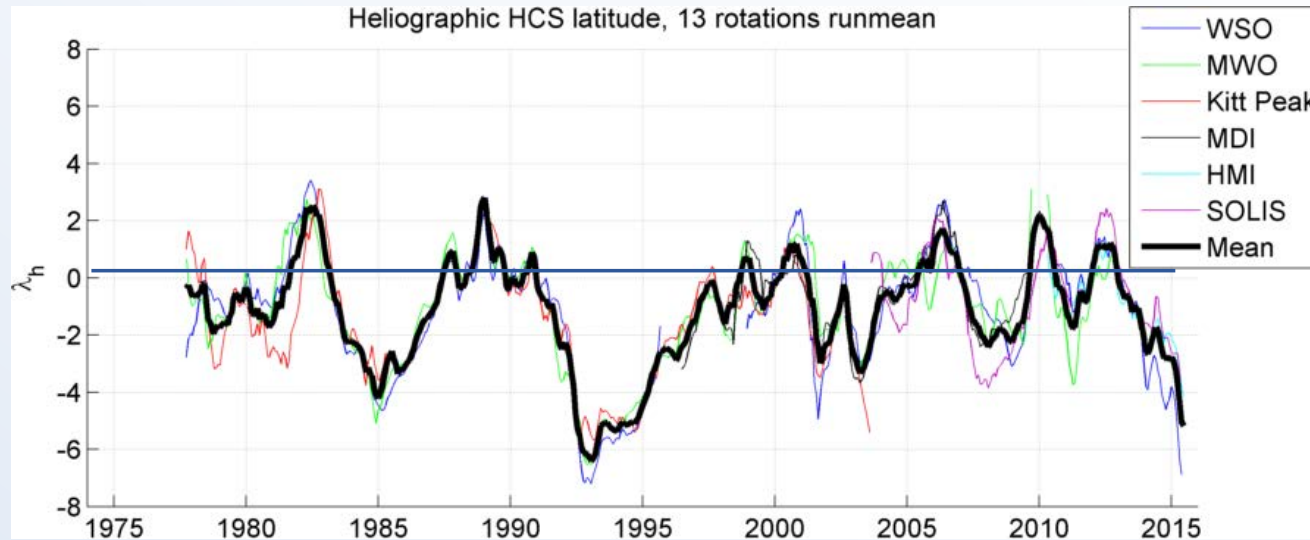
Coronal PFSS (potential field source surface) field.
Source surface is marked by dashed circle.

Heliospheric current sheet, the magnetic equator, is tilted south by 4.1° .



B. Zieger, and K. Mursula, Two-dipole model of the asymmetric Sun, J. Space Weather Space Clim., 10, 40, 10 pages, <https://doi.org/10.1051/swsc/2020041>, 2020.

HCS shift in 1977-2015



I. I. Virtanen, and K. Mursula, Photospheric and coronal magnetic fields in six magnetographs: I. Consistent evolution of the bashful ballerina, *Astron. Astrophys.*, 591, A78, 2016.

- The average heliographic latitude of the current sheet in the solar corona.
- Derived using PFSS model and six different data sets (erroneous data removed).
- **Very systematic agreement between the six different data sets.**
- **Overall, significant southward dominance during most of the time.**
- Southward shifted HCS during the declining to minimum phase of solar cycles (20,) 21, 22 and 23 (slightly less systematic) **and 24.**

Thanks

This is the End.

Yes, the End, my Friend.

Thank you for interest.

Good luck to everybody!

Actually, NOT the End

The story continues as a seminar on
Tuesday, May 9, 2023, at 1415:

Kalevi Mursula:

Relic field in the Sun:
New paradigm for Space climate

<https://oulu.zoom.us/j/67008386293>